New constructions of fundamental polyhedra in complex hyperbolic space

M. Deraux
Centre de Mathématiques
École Polytechnique
91128 Palaiseau Cedex, France
deraux@math.polytechnique.fr

E. Falbel, J. Paupert
Institut de Mathématiques
Université Pierre et Marie Curie
4, place Jussieu
F-75252 Paris, France
falbel,paupert@math.jussieu.fr

March 31, 2005

Abstract

We give a new construction of fundamental domains in $\mathbf{H}^2_{\mathbb{C}}$ for the action of the lattices in $PU(2,1)$ discovered by Mostow, some of which are non-arithmetic. The polyhedra we define have a simpler combinatorial structure than the Dirichlet domains used by Mostow and the proofs involve mostly synthetic arguments in complex hyperbolic geometry.

1 Introduction

Construction of lattices in $PU(n,1)$ has been a major challenge in the last decades. In particular, in contrast with the situation in real hyperbolic space, non-arithmetic lattices have been found only in dimensions up to three (see [M1], [DM] and [M2]).

Mostow's first examples in $PU(2,1)$ were constructed by giving explicit generators, and verifying that the corresponding groups are discrete by finding a fundamental domain for their action. In complex hyperbolic space, or in any space where sectional curvature is not constant, such an approach is bound to be at least somewhat difficult since there are no totally geodesic real hypersurfaces.

Other direct proofs of discreteness have led to domains bounded by various types of hypersurfaces, each of them adapted to the situation at hand (see the constructions in [FP], [S1]). There is a canonical construction due to Dirichlet, where the boundary of the domain is made up of bisectors, i.e. hypersurfaces equidistant from two given points. One chooses a point p_0, and considers the set F of points closer to p_0 than to any other point in its orbit under the group. It is obvious that the group is discrete if and only if F contains a neighborhood of p_0, but the set F is in general very difficult to study or describe. Such a description amounts to solving a system of infinitely many quadratic inequalities in four variables (the real and imaginary part of the coordinates in the complex 2-ball). In particular, bisector intersections are neither transverse nor connected in general.

Nevertheless, this was the original approach taken by Mostow ([M1]) to study a remarkable class of groups, $\Gamma(p, t)$ (where $p = 3, 4, 5$ and t is a real parameter). Each of these is generated by three braiding complex reflections R_1, R_2, R_3 of order p; it is contained with finite index in the group $\tilde{\Gamma}(p, t)$ generated by R_1 and the elliptic element J which conjugates R_i into R_{i+1} (see section 2.2 for further details).

There are very few values of the parameter t for which $\Gamma(p, t)$ is discrete; for these values Mostow shows discreteness using Dirichlet domains, discovered by computer experimentation. They turn out to be the intersection of the three Dirichlet domains for the finite groups $\langle R_i, R_j\rangle$ generated by only two of the generators R_i. The advantage of working with a finite group is obvious, namely one needs to solve a *finite* set of inequalities. However, the fact that the inequalities are quadratic is still an important difficulty, and in fact using current computer technology, it is fairly easy to convince oneself that Mostow's domains for these finite groups (see [M1], page 220) are incorrect. The missing faces, most of which do not contain the common fixed point of the finite group, are described in [De] (it turns out that many of the extra faces disappear when taking the intersection of the three domains for different finite groups).

Part of Mostow's mistake comes from the assumption that the Dirichlet domain for each of the finite groups Γ_{ij} is a cone with vertex given by its fixed point p_{ij}, which is far from being the case. Conical fundamental domains for finite subgroups of $U(2)$ have been constructed in [FPa], but these are not Dirichlet domains. Our constructions also naturally yield cone fundamental domains for Γ_{ij}, having eight cone faces over the eight faces in Figure 5.

The fact that these mistakes are particularly difficult to notice in Mostow's paper, and that they seem quite difficult to fix, prompted us to write a detailed argument, using more geometric techniques. Another motivation for our work is to obtain simpler domains than the ones obtained by the Dirichlet construction, by allowing totally real 2-faces, that are necessarily excluded from Dirichlet domains (see Proposition 2.5).

The presence of totally real faces is related to the fact that Mostow's groups are index two subgroups of groups generated by three involutions fixing Lagrangian totally geodesic submanifolds (see section 2.2). This observation makes them part of a large family containing infinite covolume groups (see [FK]) and all finite subgroups of $U(2)$ (see [FPa]), among which one would expect to find other lattices as well.

We construct new fundamental polyhedra $\Pi = \Pi_{p,t}$ in $\mathbf{H}^2_{\mathbb{C}}$ for the action of $\tilde{\Gamma}(p, t)$. Our fundamental domains have the same vertices as Mostow's domains, but their higher-dimensional skeletons are simpler and more natural. All our 1-faces are geodesic segments, and many (but not all) of our 2-faces are either real or complex totally geodesic submanifolds. The 3-faces are either on bisectors, or on cones over totally geodesic submanifolds. Note that this construction is related to a fundamental domain for the Eisenstein-Picard group constructed in [FP].

The main advantage, beyond the simplification of the combinatorics of the domains (see section 7), is that most verifications can be phrased in concrete geometric terms and the arguments are often completely synthetic, i.e. very few calculations are needed.

In order to prove discreteness, we show that Π and its images under the group tile complex hyperbolic space, by using the appropriate version of the Poincaré polyhedron theorem. In particular, to show that Π and $\gamma\Pi$ have disjoint interior for every nontrivial group element γ, we are reduced to showing this for a finite set of group elements, provided that we can check some detailed compatibility conditions along the codimension two faces of Π.

It turns out that only the cycles of complex geodesic faces impose conditions on the parameters, known as the Picard integrality conditions. The corresponding cycle transformations are simply complex reflections, whose angle of rotation is required to be an integer fraction of π, see Proposition 5.4. The heart of the proof consists in a careful justification (incomplete in [Pi], and not quite satisfactory in [M1]) that these are the only conditions. The main result is the following theorem (see section 2.2 for the definition of the group, and section 3 for the description of Π):

Theorem 1.1 *The group $\tilde{\Gamma}(p,t) \subset PU(2,1)$, for $p = 3,4,5$ and $|t| < \frac{1}{2} - \frac{1}{p}$, is discrete if $k = (\frac{1}{4} - \frac{1}{2p} + \frac{t}{2})^{-1}$ and $l = (\frac{1}{4} - \frac{1}{2p} - \frac{t}{2})^{-1}$ are in $\mathbb{Z}$. In that case Π is a fundamental domain with side pairings given by J, R_1, R_2, R_2R_1, R_1R_2 and the cycle relations give the following presentation of the group*

$$\tilde{\Gamma}(p,t) = \langle J, R_1, R_2 \mid J^3 = R_1^p = R_2^p = J^{-1}R_2^{-1}JR_1^{-1} = R_1R_2R_1R_2^{-1}R_1^{-1}R_2^{-1}$$
$$= (R_2R_1J)^k = ((R_1R_2)^{-1}J)^l = I\rangle.$$

The condition $|t| < \frac{1}{2} - \frac{1}{p}$ shall be referred to as *small phase shift*, following Mostow. In fact the conclusion of the theorem holds for large phase shift as well, but the combinatorics of the fundamental domains are then quite different. For the sake of brevity, we shall only sketch the corresponding changes in our fundamental domain, see section 6.

There are finitely many values of t for which the integrality conditions hold, and among the corresponding groups, seven are non arithmetic. The list is given in Remark 5.3 on page 37.

Our cone polyhedra turn out to be very convenient when proving that Π and $\gamma\Pi$ have disjoint interiors. In most cases we find a bisector B_γ that separates them (but these bisectors are certainly not all equidistant from a given point p_0, unlike in the Dirichlet construction). In order to verify that Π or $\gamma\Pi$ lies entirely on one side of B_γ, we carefully argue that it is enough to verify this on the level of its 1-skeleton. Note that verifications on the 0-skeleton would quite clearly not be enough to prove that our polyhedron is on one side of a bisector, since the two complementary components of a bisector are far from being convex.

Verifications on the 1-skeleton become relatively easy, as they amount to analyzing the intersection of a bisector with geodesic segments (see Lemma 4.2). Note that the strength of the reduction is that we only need to check the position of a finite number of geodesic segments with respect to finitely many bisectors, which in turn amounts to checking finitely many inequalities. The verifications can be done very efficiently with the aid of a computer; however our proofs are geometric and most of the time synthetic. For the case $p = 3$, the small number of calculations could in principle even be done by hand.

Going from the 1-skeleton to the 2-skeleton involves geometric arguments of general interest about the projection of totally geodesic submanifolds onto a given complex geodesic, which is usually the complex spine of the relevant bisector (see Lemma 2.1). The main point is to analyze when a geodesic projects onto a geodesic, as in Lemma 4.1. Finally, passing to the 3-skeleton is quite natural using the structure of our 3-faces, either the slice decomposition of bisectors, or the cone structure of the other faces.

The paper is organized as follows. In section 2 we review a number of geometric facts about complex hyperbolic space and bisectors, and give a description of the relevant groups. We construct our polyhedra $\Pi_{p,t}$ in section 3, and section 4 is devoted to a detailed verification that they have no self-interection and are homeomorphic to a closed ball in complex hyperbolic space.

In section 5 we prove the main theorem by verifying the conditions of the Poincaré polyhedron theorem, following the strategy outlined above. Section 6 states the modifications needed in order to treat all the cases from [M1], allowing $|t| \geq \frac{1}{2} - \frac{1}{p}$. Section 7 contains a comparison with Mostow's original fundamental domains, including some difficulties encountered with the arguments in [M1]. For the reader's convenience, the last section lists the faces of our polyhedra and their lower-dimensional skeletons.

2 Complex Hyperbolic space

We use [Go] as a general reference for this section. Let $\langle \cdot, \cdot \rangle$ be a Hermitian form of signature $(2, 1)$ on $\mathbb{C}^3$. The set of complex lines in $\mathbb{C}^3$ on which the Hermitian form is negative definite is a model of complex hyperbolic space. One can write the distance between two points as

$$\cosh(\frac{1}{2}d([x], [y])) = \frac{|\langle x, y \rangle|}{\sqrt{\langle x, x \rangle \langle y, y \rangle}} \tag{2.1}$$

The factor $\frac{1}{2}$ is chosen so as to get a metric with sectional curvature between -1 and $-\frac{1}{4}$.

More explicitly, we consider a Hermitian form $\langle z, w \rangle = z^T H \bar{w}$, where H is a Hermitian matrix of signature $(2, 1)$, and the following subsets of $\mathbb{C}^3$:

$$V_0 = \left\{ z \in \mathbb{C}^3 - \{0\} \quad : \quad \langle z, z \rangle = 0 \right\},$$

$$V_- = \left\{ z \in \mathbb{C}^3 - \{0\} \quad : \quad \langle z, z \rangle < 0 \right\}.$$

Let $\pi : \mathbb{C}^3 \setminus \{0\} \to \mathbb{C}P^2$ be the canonical projection onto the complex projective space. Then $\mathbf{H}^2_{\mathbb{C}} = \pi(V_-)$ is complex hyperbolic space. In the case where

$$H = \begin{pmatrix} 1 & 0 & 0 \\ 0 & 1 & 0 \\ 0 & 0 & -1 \end{pmatrix}$$

we obtain in non-homogeneous coordinates the complex ball

$$\mathbf{H}^2_{\mathbb{C}} = \{ \ (z_1, z_2) \in \mathbb{C}^2 \mid |z_1|^2 + |z_2|^2 < 1 \ \}.$$

The group of holomorphic isometries of $\mathbf{H}^2_{\mathbb{C}}$ is then $PU(2, 1)$ (the projectivisation of the unitary group of the Hermitian form), and the full group of isometries of complex hyperbolic space, which we denote $\widehat{PU(2, 1)}$, is obtained by adjoining just one anti-holomorphic involution.

Anti-holomorphic involutions are also called *real reflections* ($\mathbb{R}$-*reflections*) or *Lagrangian reflections*. In the ball coordinates as above an example of such a transformation is: $(z_1, z_2) \mapsto (\bar{z}_1, \bar{z}_2)$. Their fixed point set is a totally real totally geodesic submanifold which is a Lagrangian submanifold for the symplectic structure on $\mathbf{H}^2_{\mathbb{C}}$ defined by the imaginary part of the Hermitian metric.

Given a vector v with $\langle v, v \rangle = 1$, we consider the isometry of $\mathbb{C}^3$ given by

$$R_{v,\zeta}(x) = x + (\zeta - 1)\langle x, v \rangle v \tag{2.2}$$

where ζ is a complex number of absolute value one. The corresponding isometry of complex hyperbolic space is called a complex reflection; it fixes the totally geodesic subspace corresponding to the linear hyperplane $v^{\perp}$, and rotates in the normal direction by an angle θ, where $\zeta = e^{i\theta}$.

Totally geodesic subspaces of complex hyperbolic space have the following natural description.

Proposition 2.1 *The complete totally geodesic subspaces of $\mathbf{H}^2_{\mathbb{C}}$ are either geodesics, fixed subsets of complex reflections (complex lines, also called $\mathbb{C}$-planes) or fixed subsets of Lagrangian reflections (Lagrangian planes, also called $\mathbb{R}$-planes).*

The following lemma describes the projection of geometrical objects into a complex line.

Lemma 2.1 *Let π_C be the orthogonal projection of complex hyperbolic space onto a complex line C.*

1. *The image under π_C of a polygon in a complex line is either a point or another polygon such that the angles at the vertices are preserved.*

2. *The image under π_C of a polygon in a Lagrangian plane is either contained in a geodesic, or a polygon or the union of two polygons with a common vertex.*

Proof. The first item follows from the fact that the projection is holomorphic. For the second item, suppose the image of the projection is not contained in a geodesic. The projection is either a diffeomorphism, and in that case the image is another polygon, or the projection is singular at a point. That means that the differential of the projection has a non-trivial kernel. Every vector in the kernel generates a geodesic which projects to a point; in fact such a geodesic is contained in the Lagrangian and in the complex line tangent to the vector. We then claim that there is at most one of these geodesics: if there are two of them then clearly they are ultraparallel, the common orthogonal geodesic is contained in C which therefore intersects the Lagrangian in a geodesic. This would mean that the Lagrangian projects to that geodesic, which we have ruled out. Then the singular geodesic separates the Lagrangian in two and in each half the projection is a diffeomorphism.

□

Remark 2.1 One can easily show, by using coordinates with center at the intersection, that if the Lagrangian intersects the complex line its projection is either a geodesic (and in that case that geodesic is precisely the intersection) or a geodesic cone in the complex line at the intersection point.

2.1 Bisectors

Recall that the bisector equidistant from two points x_1 and $x_2 \in \mathbf{H}^2_{\mathbb{C}}$ is given by

$$B(x_1, x_2) = \{x \in \mathbf{H}^2_{\mathbb{C}} : d(x, x_1) = d(x, x_2)\} \tag{2.3}$$

In what follows we will also denote by x_1 and x_2 lifts to $\mathbb{C}^3$, by a slight abuse of notation. In view of equation (2.1), if we normalize two vectors x_1 and x_2 to have equal norms, the bisector is simply the projectivization of the set of vectors x that satisfy

$$|\langle x, x_1\rangle| = |\langle x, x_2\rangle| \tag{2.4}$$

An example in the ball model is the "standard" bisector:

$$B_0 = \{(z,t) \in \mathbf{H}^2_{\mathbb{C}} : z \in \mathbb{C}, t \in \mathbb{R}\}$$

which is equidistant from $x_1 = (0, \frac{i}{2})$ and $x_2 = (0, -\frac{i}{2})$ for instance.

A bisector is a smooth real hypersurface diffeomorphic to a ball, but it is not totally geodesic. The **complex spine** Σ of $B(x_1, x_2)$ is by definition the complex geodesic that contains x_1 and x_2. The **real spine** σ is the real geodesic in Σ that is equidistant from x_1 and x_2.

Proposition 2.2 *1.* **[Mostow]** *B is foliated by complex geodesics of the form $\pi_\Sigma^{-1}(\{p\})$, for $p \in \sigma$. These are called the* ***complex slices*** *of B.*

2. **[Goldman]** *B is the union of all the Lagrangian planes that contain its real spine σ. These are called the* ***meridians*** *of B.*

The complex slice decomposition is quite easy to understand from equation (2.4), which is equivalent to saying that $x \in (x_1 - \alpha x_2)^\perp$ for some complex number α with $|\alpha| = 1$. The hyperplanes corresponding to the orthogonal complements of $x_1 - \alpha x_2$ (whenever such a vector has positive norm), are precisely the complex slices of B.

Remark 2.2 1. The complex slice decomposition makes it clear that a bisector is uniquely determined by its real spine.

2. The Lagrangian reflection in any meridian of B fixes its real spine, hence preserves its complex spine. It must then interchange the two points x_1 and x_2. In fact if x is on the complex spine (but not on the real spine), and μ is the Lagrangian reflection in any meridian of B, then B is equidistant from x and $\mu(x)$.

The following result gives a refinement of the statement that bisectors are not totally geodesic:

Proposition 2.3 (see [Go], Theorem 5.5.1) *Let B be a bisector, and $x, y \in B$. Then the real geodesic between x and y is contained in B if and only if x and y are in either a complex slice or a meridian of B.*

2.1.1 Intersection with complex lines

In view of the slice decomposition for bisectors, it is clear that the following result is important to understand bisector intersections.

Proposition 2.4 ([M1]) *Let C be a complex geodesic that is not a complex slice of a bisector B. Then $B \cap C$ is either empty or a hypercycle in the complex geodesic.*

Recall that a hypercycle in C is a curve at constant distance from a real geodesic. In particular, unless the two bisectors share a common slice, the proposition implies that their intersection is foliated by arcs of circles. Since the complex slices map into the real spine under projection onto the complex spine, one sees that each connected component of the intersection $B_1 \cap B_2$ is a disk (indeed it fibers over an interval, with intervals as fibers). It can be proven that there are at most two connected components. If the bisectors are coequidistant, more can be said:

Proposition 2.5 *Let B_1 and B_2 be two coequidistant bisectors, i.e such that their complex spines intersect outside their real spines. Then $B_1 \cap B_2$ is diffeomorphic to a disk. If the disk is totally geodesic then it is in a common complex slice.*

A proof of this can be found in [Go]. When the intersection is not geodesic, we call it a *Giraud disk*. Observe that, in particular, the intersection of two coequidistant bisectors cannot contain a meridian. The latter fact can be seen directly: if two equidistant bisectors $B_1 = B(x_0, x_1)$ and $B_2 = B(x_0, x_2)$ share a meridian with $\mathbb{R}$-reflection μ, then as we have just seen μ exchanges on one hand x_0 and x_1, and on the other x_0 and x_2, so that the bisectors are equal.

The following lemma characterizes complex lines intersecting a bisector in a geodesic.

Lemma 2.2 *Let C be a complex geodesic, and let B be a bisector with real spine σ. Suppose that C is not a complex slice of B, and $C \cap B$ is non empty. Then $C \cap B$ is a geodesic if and only if the extensions to projective space of C and σ intersect.*

Proof. Let Σ be the complex spine of B, which is the complex geodesic containing the real geodesic σ.

1. Suppose Σ and C intersect in $H^2_{\mathbb{C}}$. If the real spine goes through their intersection, then taking the origin of our ball coordinates to be that intersection point makes the equation of B linear, hence the intersection is a line through the origin, which is a geodesic.

   Conversely, if C intersects Σ outside of σ, we still take coordinates centered on σ, so that the intersection is again given by a straight line. If this line were a geodesic, it would have to be contained in a meridian of B, but then it would intersect σ in projective space (but two complex projective lines intersect in exactly one point).

2. The case where Σ and C intersect on $\partial H^2_{\mathbb{C}}$ is similar to the previous one.

3. Suppose Σ and C intersect outside of $H^2_{\mathbb{C}} \cup \partial H^2_{\mathbb{C}}$. Then these two complex geodesics have a common perpendicular complex geodesic D. We may assume that Σ is given by $z_2 = 0$, that C is $z_2 = c$, $c \neq 0$ and D is $z_1 = 0$. The real spine is either a straight line or a circle, depending on whether or not it goes through the origin.

   Note that the intersection $B \cap C$ is the intersection with C of the inverse image of σ under the linear projection $(z_1, z_2) \mapsto z_1$. Remembering that real geodesics in complex geodesics are orthogonal to the boundary, we see that $B \cap C$ is a geodesic if and only if σ is a straight line. This in turn is equivalent to saying that C and σ intersect in projective space (since any intersection would have to take place at infinity in $\mathbb{C}^2$).

□

2.1.2 Intersection with Lagrangian planes

The intersections of Lagrangians with bisectors have the following general property (which expresses the fact that a suitable normalisation of the coordinates gives a quadratic equation for such an intersection):

Proposition 2.6 *Let L be a Lagrangian which is not a meridian of the bisector B. Then $B \cap L$ is a conic in L.*

Note that singular conics can occur (two intersection lines). We describe that situation more explicitly. Using the ball coordinates, the Hermitian metric is written at $p = (b, 0)$ with b real as (see [Go])

$$\begin{bmatrix} \frac{1}{(1-b^2)^2} & 0 \\ 0 & \frac{1}{(1-b^2)} \end{bmatrix}$$

Lemma 2.3 *Consider coordinates of the standard bisector $\{(z,t),\ z \in \mathbb{C},\ t \in \mathbb{R}\}$, at a point $p = (b, 0)$ with $b \in \mathbb{R}$ and let two tangent vectors $v_1 = (z_1, t_1)$ and $v_2 = (z_2, t_2)$ be in T_pB.*

1. *v_i is tangent to a meridian if and only if $z_i \in \mathbb{R}$*

2. *v_1 and v_2 are tangent to a common Lagrangian if and only if $z_1\bar{z}_2 \in \mathbb{R}$.*

Proof. The first item is obvious. For the second, we need $iv_1 \perp v_2$. Computing, using the form of the metric defined above at the point $(b, 0)$,

$$g(iv_1, v_2) = Re\langle iv_1, v_2\rangle = Re\langle (iz_1, it_1), (z_2, t_2)\rangle = Re\left(iz_1\bar{z}_2\frac{1}{(1-b^2)^2} + it_1t_2\frac{1}{(1-b^2)}\right)$$

we see that the Hermitian product is purely imaginary if and only if $z_1\bar{z}_2 \in \mathbb{R}$. $\square$

Proposition 2.7 *Suppose the tangent space to a Lagrangian L is contained in the tangent space to a bisector B, that is $T_pL \subset T_pB$. Then*

1. *$L \subset B$ is a meridian or*

2. *$L \cap B$ is the union of two geodesics passing through p, one being in a meridian and orthogonal to a slice which contains the other one.*

Proof. Follows from the lemma and proposition above. If L is not contained in B we first observe that the tangent space T_pL in the coordinates of the lemma contains the vector $(0, t)$ which is tangent to the meridian passing through $p = (b, 0)$. The geodesic along that vector is contained in both the meridian and L. Analogously, the vector $(z, 0)$ is tangent to the slice and the geodesic defined by it belongs to the slice and to L. The above proposition implies that there can be no more intersection. $\square$

Lemma 2.4 *Let g be a geodesic in a meridian of a bisector B, ultraparallel to its real spine. Then there exists a unique slice of B which is othogonal to g; moreover it is orthogonal to the complex geodesic containing g.*

Proof. Observe that in the meridian there exists a unique geodesic orthogonal to the real spine which is also orthogonal to g. The lemma follows from the fact that orthogonal geodesics in a Lagrangian plane are contained in orthogonal complex geodesics. $\square$

Proposition 2.8 *Let B be a bisector with real spine σ, and L a Lagrangian not contained in B. Suppose $L \cap B$ contains a geodesic g which is in a meridian of B but not in a slice.*

- *If g is ultraparallel to σ then $L \cap B$ contains another geodesic which is in a complex slice of B.*
- *If g intersects σ in $\mathbf{H}^2_{\mathbb{C}} \cup \partial \mathbf{H}^2_{\mathbb{C}}$ then $L \cap B = g$.*

Proof. In the first case, by the above lemma, there exists a unique slice of B orthogonal to the complex geodesic containing g. This implies that L also intersects that slice in a geodesic. In the second case, by Proposition 2.7, we can exclude a singular intersection because g is not orthogonal to any slice. To show that there is only one component in the intersection, in the case where g intersects σ in $\mathbf{H}^2_{\mathbb{C}}$ we can use ball coordinates such that both the bisector and the Lagrangian are linear. In the parallel case we observe that there is a point p at infinity belonging to the boundary of both σ and L. If $L \cap B$ were to contain a point outside of g, then the geodesic joining that point to p would belong to B and L; there would then exist a complex slice of B having two points in L, therefore $L \cap B$ would contain another geodesic intersecting g, which is a contradiction.

$\square$

We also need the following corollary to Proposition 2.7:

Proposition 2.9 *Fix four points in $\mathbf{H}^2_{\mathbb{C}}$. If three triples of these points are contained in Lagrangian planes then the four are contained in a common Lagrangian plane.*

Proof. First observe that the four triples are in fact contained in Lagrangians. Indeed, it can easily be seen (as in [Go] pg. 219), that the Cartan angular invariants of various triples among four points $x_1, x_2, x_3, x_4 \in \mathbf{H}^2_{\mathbb{C}}$ satisfy the following relation:

$$\mathbb{A}(x_1, x_2, x_3) + \mathbb{A}(x_1, x_3, x_4) = \mathbb{A}(x_1, x_2, x_4) + \mathbb{A}(x_2, x_3, x_4)$$

Consider then the tetrahedron formed by the four points. Taking opposite edges as real spines of two bisectors we obtain that the intersection contains at least the other four edges. Using Proposition 2.7 we conclude that if the Lagrangians do not coincide then there exists one of the faces with all edges meeting at right angles, which is a contradiction. $\square$

2.2 The group $\Gamma(p, t)$

The most natural description of a complex reflection group is done by means of a Coxeter diagram, where the nodes correspond to generating reflections, and the edges translate into braiding relations between the generators. In the case of complex reflection groups, there is an extra parameter attached to each loop in the diagram, the so-called phase shift. More details on the general case can be found in [M1] or [C], but for the sake of brevity we only discuss the following special case.

Consider the groups with Coxeter diagrams of the form

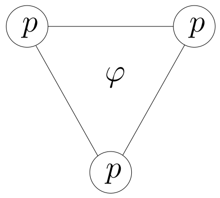

for $p = 3$, 4 or 5. Each such group is generated by three complex reflections R_1, R_2 and R_3 of order p, satisfying the braid relation

$$R_i R_j R_i = R_j R_i R_j \tag{2.5}$$

We write the mirror of R_j as $e_j^{\perp}$ (take $v = e_j$ and $\zeta = e^{2\pi i/p}$ in equation (2.2)). We may assume after rescaling the vectors e_i that $\langle e_i, e_i \rangle = 1$ and $\langle e_1, e_2 \rangle = \langle e_2, e_3 \rangle = \langle e_3, e_1 \rangle$. The braid relation imposes a condition on the angle between the mirrors of the generating reflections, which translates as

$$|\langle e_i, e_j \rangle| = \frac{1}{2 \sin \dfrac{\pi}{p}} \tag{2.6}$$

In what follows we shall write $\alpha = 1/2 \sin \frac{\pi}{p}$.

The phase shift φ that appears in the above diagram corresponds to specifying the common value of the argument of the inner products $\langle e_i, e_{i+1} \rangle$, specifically we take

$$\langle e_i, e_{i+1} \rangle = -\alpha\varphi \tag{2.7}$$

where $|\varphi| = 1$. We follow Mostow's notation and write $\varphi^3 = e^{\pi i t}$, and denote the corresponding group by $\Gamma(p, t)$.

In the basis $\{e_1, e_2, e_3\}$, the matrix for the Hermitian form is given by

$$H = \begin{pmatrix} 1 & -\alpha\varphi & -\alpha\overline{\varphi} \\ -\alpha\overline{\varphi} & 1 & -\alpha\varphi \\ -\alpha\varphi & -\alpha\overline{\varphi} & 1 \end{pmatrix} \tag{2.8}$$

The existence of a triple of positive vectors e_i satisfying (2.7) is equivalent to the requirement that H be of signature $(2, 1)$, which in turn is equivalent to

$$|t| < 3(\frac{1}{2} - \frac{1}{p}) \tag{2.9}$$

In what follows, we shall always use coordinates in this basis and the Hermitian form (2.8).

The linear transformation

$$J = \begin{pmatrix} 0 & 0 & 1 \\ 1 & 0 & 0 \\ 0 & 1 & 0 \end{pmatrix} \tag{2.10}$$

is clearly an isometry, which is a regular elliptic element fixing $p_0 = [1,1,1]^T$. Moreover there are three natural antiholomorphic isometric involutions σ_{ij}, given by complex conjugation of the coordinates followed by exchanging two of the standard basis vectors. For instance,

$$\sigma_{12} : [x_1, x_2, x_3]^T \mapsto [\overline{x}_2, \overline{x}_1, \overline{x}_3]^T \tag{2.11}$$

We will denote by L_{ij} the fixed point set of σ_{ij}, which is a Lagrangian plane by proposition 2.1.

One checks that R_1 is given in the basis $\{e_1, e_2, e_3\}$ by the following matrix, where $\eta = e^{\pi i/p}$,

$$R_1 = \begin{pmatrix} \eta^2 & -\eta i\overline{\varphi} & -\eta i\varphi \\ 0 & 1 & 0 \\ 0 & 0 & 1 \end{pmatrix} \tag{2.12}$$

Note that J conjugates R_i into R_{i+1} where indices are taken modulo 3, so that the matrices for R_2 and R_3 are easily deduced from the matrix above.

The condition that $p < 6$ is equivalent to requiring that the mirrors of two reflections R_i, R_j intersect in the ball, in a point denoted by p_{ij}. The common fixed point of R_1 and R_2 can be written as

$$p_{12} = \begin{bmatrix} \alpha\varphi + \alpha^2\overline{\varphi}^2 \\ \alpha\overline{\varphi} + \alpha^2\varphi^2 \\ 1 - \alpha^2 \end{bmatrix} \tag{2.13}$$

and the other p_{ij} are deduced by applying the isometry J.

We study the group $\tilde{\Gamma}(p,t)$ generated by J and R_1. It is instructive to decompose these generators as a product of antiholomorphic involutions:

$$\begin{cases} J = \sigma_{12}\sigma_{23} \\ R_1 = \sigma_{23}\tau \end{cases} \tag{2.14}$$

where the σ_{ij} are as in (2.11), and τ is by definition $\sigma_{23}R_1$. We shall write $\hat{\Gamma}(p,t)$ for the group generated by σ_{12}, σ_{23} and τ. Note that the subgroup $\tilde{\Gamma}(p,t) \subset \hat{\Gamma}(p,t)$ is the index two subgroup of holomorphic elements.

We write L_{ij} and L_τ for the fixed point set of σ_{ij} and τ, respectively.

Proposition 2.10 *The Lagrangians fixed by the generating antiholomorphic involutions intersect as follows:*

1. *$L_{12} \cap L_{23}$ is the isolated fixed point p_0 of J.*
2. *$L_{12} \cap L_\tau$ is the isolated fixed point p_1 of JR_1.*
3. *$L_{23} \cap L_\tau$ is a geodesic g_1, contained in the mirror of R_1.*

Proof. The first part follows from the definition of J. In order to get the second, note that JR_1 has three distinct eigenvalues, its characteristic polynomial being given by $-(\lambda+\eta i\overline{\varphi})(\lambda^2+\eta i\varphi)$. The eigenvector with negative norm is the one corresponding to $\sqrt{-\eta i\varphi} = e^{\pi i(\frac{1}{4}-\frac{1}{2p}-\frac{t}{6})}$ for $t > -(\frac{1}{2}-\frac{1}{p})$, and corresponding to $-\eta i\overline{\varphi}$ otherwise.

We now prove part 3. Since $\sigma_{23}e_1 = e_1$, σ_{23} preserves the mirror of R_1 and this implies that L_{23} intersects the mirror in a geodesic (cf. [FPa]). $\square$

We wish to use these three Lagrangians and their intersections, of dimension 0, 1 and 2, as building blocks for a fundamental polyhedron. The first observation is that these objects define a 3-dimensional object, namely the bisector B_1 having g_1 as its real spine. This bisector then has $Fix(R_1)$ as complex spine, L_{23} and L_τ as meridians, and contains the points p_0 and p_1 so it is indeed well adapted to our configuration.

We collect the groups we introduced above in the following

Definition 2.1 *For any integer p and $|t| < 3(\frac{1}{2} - \frac{1}{p})$ define*

- $\hat{\Gamma}(p,t) = \langle \sigma_{12}, \sigma_{23}, \tau \rangle$
- $\tilde{\Gamma}(p,t) = \langle R_1, J \rangle \subset \hat{\Gamma}(p,t)$ *of index two.*
- $\Gamma(p,t) = \langle R_1, R_2, R_3 \rangle \subset \tilde{\Gamma}(p,t)$,

where $R_1 = \sigma_{23}\tau$, $J = \sigma_{12}\sigma_{23}$ and $R_2 = JR_1J^{-1}$, $R_3 = J^2R_1J^{-2}$.

Note that the index of $\Gamma(p,t)$ in $\tilde{\Gamma}(p,t)$ could be one or three. Although we are not going to use the next proposition, we observe that using the main theorem we can decide, in certain cases, what the index is.

Proposition 2.11 (cf. [M1] lemma 16.1 pg. 244) *Let p and t as in Theorem 1 be such that $k = (\frac{1}{4} - \frac{1}{2p} + \frac{t}{2})^{-1}$ and $l = (\frac{1}{4} - \frac{1}{2p} - \frac{t}{2})^{-1}$ are in $\mathbb{Z}$. Then $\Gamma(p,t) \subset \tilde{\Gamma}(p,t)$ is an index 3 subgroup if k and l are both divisible by 3 and otherwise the groups are equal.*

Proof. Clearly, the quotient $\tilde{\Gamma}(p,t)/\Gamma(p,t)$ is represented by the class of J. From the main theorem we obtain the presentation with relation $(R_2R_1J)^k = I$, so

- $(R_2R_1J)^k = (R_2R_1R_3)^{2m}$ if $k = 3m$
- $(R_2R_1J)^k = (R_2R_1R_3)^{2m}R_2R_1J$ if $k = 3m+1$
- $(R_2R_1J)^k = (R_2R_1R_3)^{2m+1}R_2J^2$ if $k = 3m+2$

Therefore J is generated by R_1, R_2, R_3 if 3 does not divide k. Using the relation $((R_1R_2)^{-1}J)^l = I$ we obtain an analogous result for l. □

2.3 A canonical hexagon

Let B_1 be the bisector with real spine g_1, the geodesic where L_{23} and L_τ intersect. Note that its complex spine is by construction the mirror of the complex reflection R_1, and the Lagrangians L_{23} and L_τ are two of its meridians. In particular, it also contains the points $p_0 = L_{12} \cap L_{23}$ and $p_1 = L_{12} \cap L_\tau$ (see Proposition 2.10).

The bisector B_1 can also be described as being equidistant from two understood points. Indeed the isometry σ_{23}, which is the involution in a meridian of B_1, sends p_{12} to p_{31}. This implies that B_1 is equidistant from p_{12} and p_{31} (see Remark 2.2).

Recall that we would like to construct a 3-face of a fundamental domain on B_1. We need this face to intersect "well" with its neighbors, i.e. its images under short words in the group. This leads us to explore the intersection of the whole bisector B_1 with some of its images. Now R_1 stabilizes B_1 (in fact each slice is stabilized), and J cyclically permutes

$$B_1,\ B_2 := J(B_1),\ B_3 := J^2(B_1)$$

We thus study the intersection $S_\eta = B_1 \cap J(B_1)$.

The surface S_η is by construction equidistant from the three fixed points p_{12}, $p_{23} = Jp_{12}$ and $p_{31} = J^2 p_{12}$. This also makes it apparent that S_η is the intersection of *any two* among the three bisectors B_1, B_2 and B_3.

Proposition 2.12
- *S_η is a smooth non totally geodesic disk.*
- *S_η contains 6 geodesics, arranged in a hexagon with right angles.*

The extension to projective space of the hexagon S_η is shown in Figure 1. Note that the hexagon appears already in Mostow but not as a face (see figure 14.1 in page 236 in [M1]). In his notation the six vertices are $s_{12}, \tilde{s}_{13}, s_{23}, \tilde{s}_{21}, s_{31}, \tilde{s}_{32}$ and are given by

$$s_{12} = \begin{bmatrix} \overline{\eta} i\varphi \\ \overline{\eta} i\overline{\varphi} \\ 1 \end{bmatrix}, \quad \tilde{s}_{21} = \begin{bmatrix} -\eta i\varphi \\ -\eta i\overline{\varphi} \\ 1 \end{bmatrix} \tag{2.15}$$

and $s_{23} = Js_{12}$, $s_{31} = Js_{23}$, $\tilde{s}_{32} = J\tilde{s}_{21}$, $\tilde{s}_{13} = J\tilde{s}_{32}$

The next section, which provides a proof of Proposition 2.12, is devoted to a more detailed analysis of this situation. It is somewhat technical and can be skipped during a first read; the reader can simply assume Proposition 2.12 and refer to Figure 1.

2.4 Computing the vertices of the hexagon

We now prove Proposition 2.12. The first part follows from Proposition 2.5. Indeed, the bisectors B_i and B_j are co-equidistant, since their complex spines intersect at the point p_{ij}.

In the following arguments, we shall often refer to intersections taking place in complex *projective* space rather than hyperbolic space. We denote by $\tilde{S}_\eta$ the extension to projective space of S_η, which is the set of lines $[x]$ (not necessarily negative definite with respect to the Hermitian form) such that

$$|\langle x, p_{12}\rangle| = |\langle x, p_{23}\rangle| = |\langle x, p_{31}\rangle| \tag{2.16}$$

It is readily checked that $\tilde{S}_\eta$ is a torus in projective space (cf. [Go], Lemma 8.3.4). Similarly, $\tilde{\sigma}_j$ denotes the extension to projective space of the real spine σ_j. It is simply the circle parameterized by $p_{ij} - \alpha p_{jk}$, $|\alpha| = 1$. It is clear from the definitions that $[x] \in \tilde{S}_\eta$ is equivalent to saying that x is orthogonal to two vectors of the form $p_{ij} - \alpha_i p_{ki}$ and $p_{ij} - \alpha_j p_{jk}$, $|\alpha_i| = |\alpha_j| = 1$.

The second statement follows from the following observations:

Proposition 2.13 *1. For each i, there are precisely two complex slices of B_i that intersect S_η in a geodesic. We choose vectors v_{jik} and v_{kij} polar to these two complex slices.*

2. *The vectors v_{jik} and v_{kij} correspond to the two intersection points of $\tilde{\sigma}_i$ and $\tilde{S}_\eta$ in projective space.*

3. $v_{ijk} \perp v_{jik}$ *and* $v_{ijk} \perp v_{ikj}$.

4. *The union of any two adjacent sides of the hexagon is the intersection with S_η of a meridian of one of the three bisectors B_i.*

The reader should keep Figure 1 at hand when reading the proof of the proposition. The picture of $\tilde{S}_\eta$ is drawn using spinal coordinates on $B_1 \cap B_2$, so that the complex slices of B_1, B_2 and B_3 intersect $\tilde{S}_\eta$ in vertical, horizontal, and slope one lines respectively.

Proof. Lemma 2.2 implies that any slice of B_i that intersects S_η in a geodesic must intersect both $\tilde{\sigma}_j$ and $\tilde{\sigma}_k$ in projective space. By the slice decomposition, their points of intersection with the slice are orthogonal to some vector $z \in \tilde{\sigma}_i$. z is clearly contained in $\tilde{S}_\eta$, since it is orthogonal to two points from two different extended real spines.

Hence the slices C_i of B_i that intersect S_η in a geodesic are polar to points of intersection $\tilde{\sigma}_i \cap \tilde{S}_i$. Now σ_i is not contained in B_j for $j \neq i$, and it intersects (the extension) of B_j (hence $\tilde{S}_j$) in at most two points.

We now describe the intersection points $\tilde{\sigma}_j \cap \tilde{S}_\eta$. The corresponding six points appear already in [M1], and are denoted v_{ijk} (where all indices are distinct among 1, 2 and 3). We give the coordinates of two of them, the other ones being deduced by applying J and the according cycle in the indices:

$$v_{123} = \begin{bmatrix} -\eta i\overline{\varphi} \\ 1 \\ \overline{\eta} i\varphi \end{bmatrix}, \quad v_{321} = \begin{bmatrix} \overline{\eta} i\overline{\varphi} \\ 1 \\ -\eta i\varphi \end{bmatrix} \tag{2.17}$$

These vectors have geometric meaning, namely v_{ijk} can be checked to be orthogonal to the mirrors of a complex reflections given by $J^{\pm 1} R_j R_k$, where the power is 1 if $k = j + 1$ and -1 if $k = j - 1$.

Using (2.13), one verifies that

$$p_{12} + \eta i\varphi p_{23} = \alpha^2(\eta^2\varphi^2 + \overline{\eta} i\overline{\varphi}) v_{123} \tag{2.18}$$
$$p_{12} - \overline{\eta} i\varphi p_{23} = \alpha^2(\overline{\eta}^2\varphi^2 - \eta i\overline{\varphi}) v_{321} \tag{2.19}$$

which implies that v_{123} and v_{321} are indeed on the extended real spine of B_2. Similarly, applying J, we see that v_{ijk} is on the extended real spine of B_j. Another unenlightening computation yields

$$\langle v_{123}, p_{12} \rangle = \overline{\eta} i\varphi\kappa \tag{2.20}$$
$$\langle v_{123}, p_{23} \rangle = -\eta i\overline{\varphi}\kappa \tag{2.21}$$
$$\langle v_{123}, p_{31} \rangle = \kappa \tag{2.22}$$

$$\langle v_{321}, p_{12} \rangle = -\eta i\varphi\kappa \tag{2.23}$$
$$\langle v_{321}, p_{23} \rangle = \overline{\eta} i\overline{\varphi}\kappa \tag{2.24}$$
$$\langle v_{321}, p_{31} \rangle = \kappa \tag{2.25}$$

where $\kappa = \det(H) = 1 - 3\alpha^2 - \alpha^3(\varphi^3 + \overline{\varphi}^3)$. Note that all the complex numbers from equation (2.20) have the same absolute value, so v_{123} and v_{321} are in $\tilde{S}_\eta$, see (2.16). The above result remains true for any v_{ijk} simply by applying the 3-cycle J.

This proves parts 1 and 2 of the proposition. We now check the orthogonality claim, namely that two successive spikes of the star of Figure 1 are represented by orthogonal vectors. We only check that v_{321} and v_{312} are orthogonal (the other orthogonality properties are easily deduced from this one). This follows at once from direct calculation, but a better interpretation is that the group contains a number of pairs of commuting complex reflections. Namely, $v_{312}^\perp$ is the mirror of $J^{-1}R_1R_2$, and $v_{321}^\perp$ is the mirror of JR_2R_1. Now these two mirrors are orthogonal, since

$$(J^{-1}R_1R_2)(JR_2R_1) = J^{-1}R_1JJ^{-1}R_2JR_2R_1 = R_3R_1R_2R_1 \tag{2.26}$$

$$(JR_2R_1)(J^{-1}R_1R_2) = JR_2J^{-1}JR_1J^{-1}R_1R_2 = R_3R_2R_1R_2 \tag{2.27}$$

and these two are equal because of the braiding relation (these commutation relations become more transparent in the description of the groups given in [DM]).

It can be checked that, for $|t| < \frac{1}{2} - \frac{1}{p}$, all v_{ijk} are positive vectors, so that $v_{312}^\perp \cap v_{321}^\perp$ is a negative line. The corresponding point in complex hyperbolic space is denoted by s_{12} in [M1]. Similarly, there is a point $\tilde{s}_{21}$ which can be described as $v_{123}^\perp \cap v_{213}^\perp$.

One can compute explicit homogeneous coordinates for these points, and obtain expression (2.15). Coordinates for the other four vertices of the hexagon are easily obtained from s_{12} and $\tilde{s}_{21}$ by applying the symmetry J, namely $s_{23} = Js_{12}$, $s_{31} = Js_{23}$, $\tilde{s}_{32} = J\tilde{s}_{21}$, $\tilde{s}_{13} = J\tilde{s}_{32}$.

It follows from the above orthogonality property that the complex geodesics that contain two successive sides of the hexagon are orthogonal, hence the real geodesics themselves must be orthogonal. The orthogonality of the complex geodesics also implies that two successive sides of the hexagon are contained in a totally real 2-plane, which must then be a meridian of one of the three bisectors intersecting in the Giraud disk (indeed it contains two points of its extended real spine). This gives part 4. □

3 Description of a fundamental polyhedron Π in $\mathbf{H}^2_{\mathbb{C}}$

Our fundamental domain is a polyhedron Π constructed as a cone at a point p_{12} over the union of two 3-cells named H and H' intersecting in a hexagonal 2-cell η.

3.1 The core hexagon

In order to construct the first 3-faces of the fundamental domain we recall that the intersection $S_\eta = B_1 \cap J(B_1)$ is a topological disc which contains 6 geodesics, arranged along a hexagon with right angles, see Proposition 2.12. We thus define a 2-face η of our polyhedron to be the part of the surface S_η bounded by the hexagon; this 2-face is contained in two 3-faces which we now define, H in B_1 and H' in $B_1' = J(B_1)$. Here in and in what follows, we denote

$$B_1,\ B_1' := J(B_1),\ B_1'' := J^2(B_1)$$

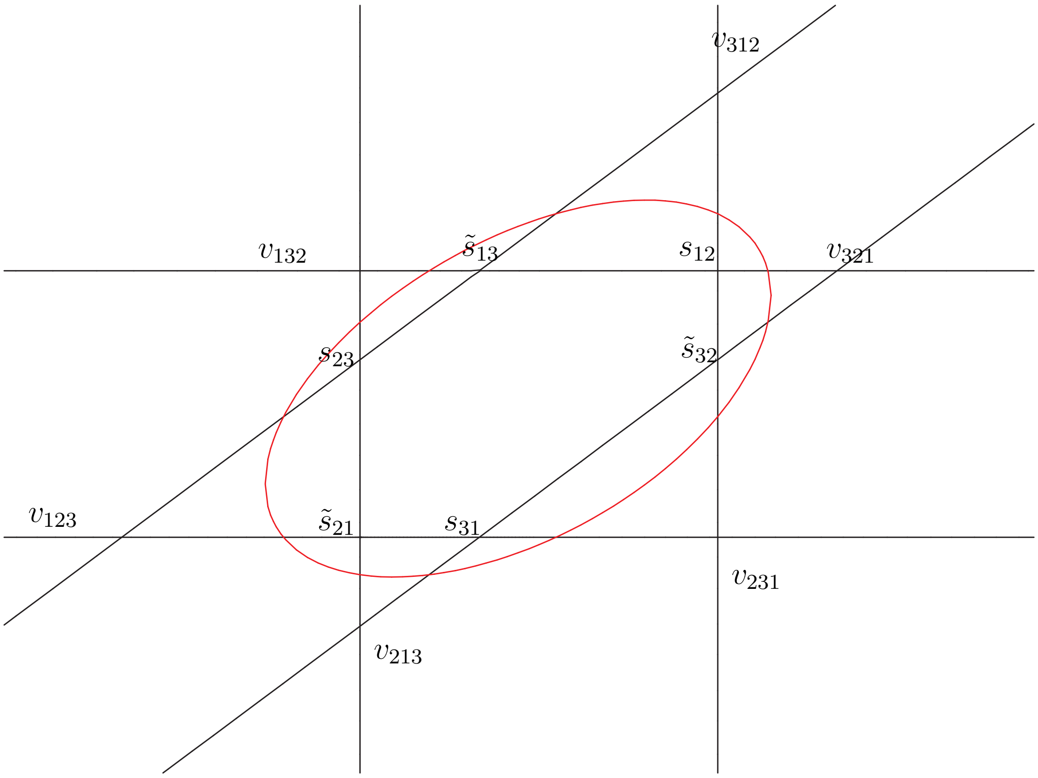

Figure 1: A right angled geodesic hexagon on the Giraud disk $B_1 \cap B_2 \cap B_3$, for $t = 1/18$. The figure shows a neighborhood of the disk in its torus extension to projective space.

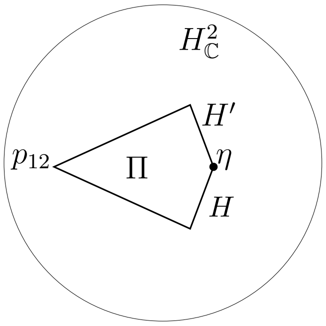

Figure 2: A schematical view of the fundamental domain. The two 3-faces H and H' intersect in a 2-face (an hexagon) η. The domain is a geodesic cone from p_{12}.

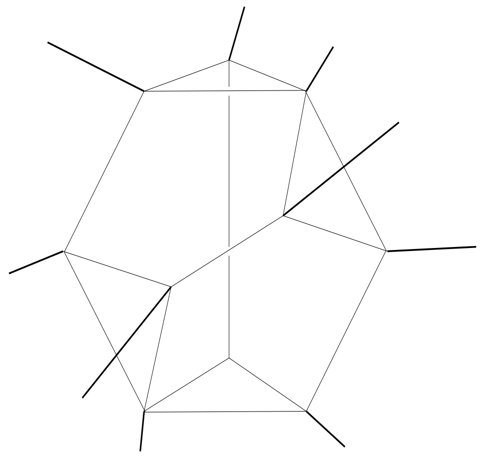

Figure 3: The boundary of the fundamental domain is a sphere divided into 10 cells. The cone point p_{12} is represented at infinity and only two of the 3-cells are finite. They correspond to H and H' and intersect in a hexagon. There are 4 pentagonal prisms and 4 tetrahedra containing p_{12} as a vertex. The 1-cells are all geodesics.

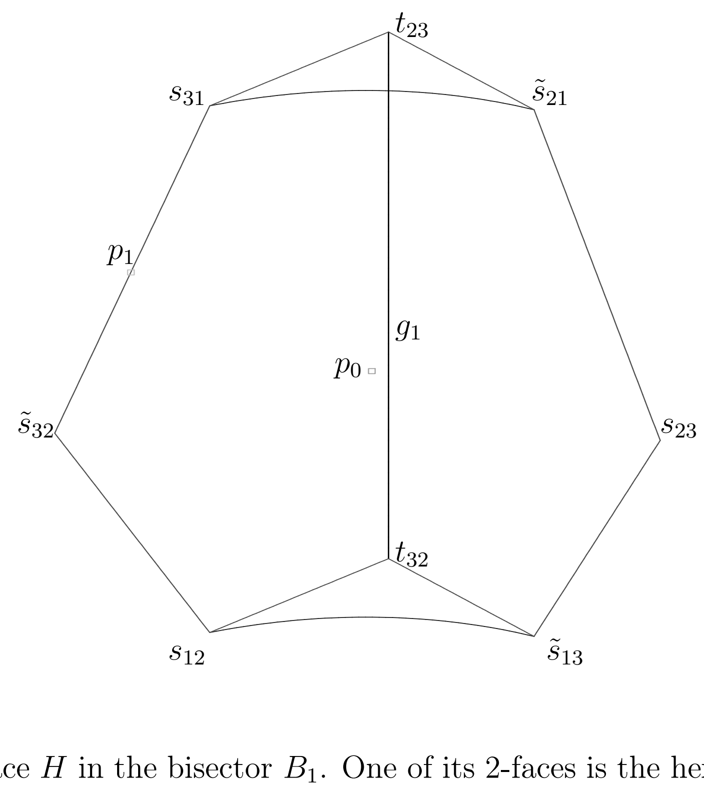

Figure 4: The 3-face H in the bisector B_1. One of its 2-faces is the hexagon η contained in the intersection $B_1 \cap J(B_1)$.

3.2 The 3-faces H and H'

We first take a closer look at the position of the hexagon in the first bisector B_1. We have:

- s_{12}, s_{31} and $\tilde{s}_{32}$ are in the meridian L_τ.
- $\tilde{s}_{13}, s_{23}$ and $\tilde{s}_{21}$ are in the meridian $R_1(L_\tau)$.
- s_{31} and $\tilde{s}_{21}$ are in a common slice.
- s_{12} and $\tilde{s}_{13}$ are in a common slice.

The situation can be seen on Figure 4 , where we use coordinates on B_1 adapted to the bisector structure, in the sense that the (real) spine is the vertical axis, slices are horizontal planes and meridians are vertical planes containing the axis. We call such coordinates *spinal coordinates* on B_1.

We are now ready to complete the 3-face H by adding two vertices, t_{23} and t_{32} in Mostow's notation. They are given by the projection onto the spine of B_1 of the two slices containing the pairs $(s_{31}, \tilde{s}_{21})$, and $(s_{12}, \tilde{s}_{13})$ respectively. An elementary computation gives the following formulas:

$$t_{23} = \begin{bmatrix} \alpha|\varphi - \eta i\overline{\varphi}^2|^2 \\ \varphi - \eta i\overline{\varphi}^2 \\ \overline{\varphi} + \overline{\eta} i\varphi^2 \end{bmatrix}, \quad t_{32} = \begin{bmatrix} \alpha|\overline{\varphi} - \eta i\varphi^2|^2 \\ \varphi + \overline{\eta} i\overline{\varphi}^2 \\ \overline{\varphi} - \eta i\varphi^2 \end{bmatrix} \tag{3.1}$$

We then enclose H by adding four 2-faces:

- two $\mathbb{C}$-planar geodesic triangles, $\tau_{11} = (t_{23}, s_{31}, \tilde{s}_{21})$ in the "top" slice and $\tau_{21} = (t_{32}, s_{12}, \tilde{s}_{13})$ in the "bottom" slice,
- two $\mathbb{R}$-planar geodesic right-angled pentagons, $\pi_1 = (t_{23}, s_{31}, \tilde{s}_{32}, s_{12}, t_{32})$ in the meridian L_τ, and $\pi_2 = (t_{23}, \tilde{s}_{21}, s_{23}, \tilde{s}_{13}, t_{32})$ in the meridian $R_1(L_\tau)$.

It is natural to construct this wedge from the spine g_1 because R_1 acts on the bisector B_1 by rotation around its spine. These five 2-faces enclose a region in B_1 which is our first 3-face H. Now the next face H' is easily derived: we simply consider $H' = J(H)$ in $B_1' = J(B_1)$. This new face, isometric to H, is glued to H along the 2-face η (with a rotation of $\frac{2\pi}{3}$ in the orientation of the picture) and it only has two new vertices $t_{31} = J(t_{23})$ and $t_{13} = J(t_{32})$ which are on the spine of B_1'.
We have thus closed the 2-face η in the sense that it belongs to two 3-faces; we eventually want to close all the 2-faces we have introduced, which is what we now do.

3.3 The whole polyhedron Π

Recall from section 2.2 that p_{12} is the intersection of the mirrors of R_1 and R_2 (see equation 2.13). Alternatively, it can be seen as the intersection of the complex spines of the two bisectors we have used so far, B_1 and B_1'.

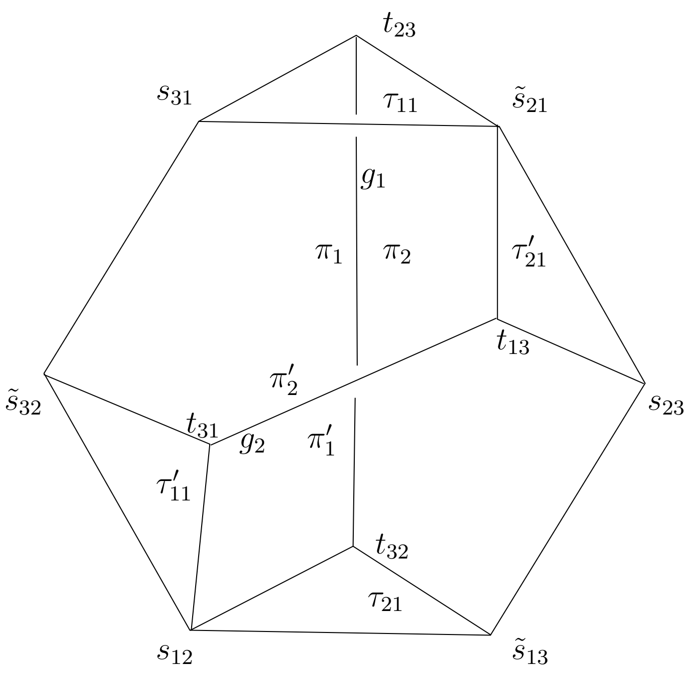

Figure 5: The core part $H \cup H'$ in $B_1 \cup B'_1$. The pentagonal 2-cells π_1 and π_2 contain the spine g_1 and π'_1 and π'_2 contain the spine g_2. The side pairing transformation which interchanges H and H' is J.

We then construct our polyhedron Π as the geodesic cone over the "core" part $H \cup H'$ from the point p_{12}. We use the notation:

$$Cone(\alpha) = \bigcup_{q \in \alpha} [p_{12}q]$$

where $[pq]$ denotes the geodesic segment from p to q. So that

$$\Pi := Cone(H \cup H')$$

This is analogous to the construction in [FP] for the Eisenstein-Picard modular group, where the cone vertex was at infinity.
With this construction, the interior of Π is the cone over the interior of $H \cup H'$, and its boundary is the cone over the boundary of $H \cup H'$, together with $H \cup H'$. Thus the boundary of Π consists in ten 3-faces: H, H' and eight faces of two combinatorial types, tetrahedra (cones over a triangle) and pentagonal pyramids (cones over a pentagon). We will see in fact that these two types are also geometrically different, because the tetrahedra live in bisectors whereas the pentagonal pyramids do not.
What is less obvious, and which we leave to the next section, is that this construction does not yield any unwanted intersection between the faces. We first describe the remaining 3-faces.

3.4 The remaining 3-faces

3.4.1 Description of a tetrahedron

The "top" and "bottom" triangles τ_{11} and τ_{21} are not isometric (unless $t = 0$), however the tetrahedra based on them have the same structure so that we need only describe the tetrahedron

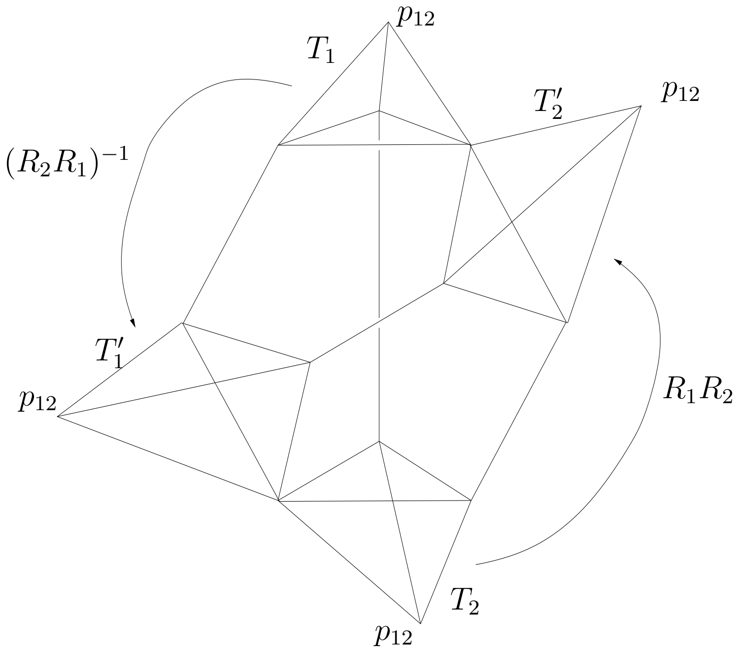

Figure 6: The 4 tetrahedra in the boundary of the polyhedron Π actually have the common vertex p_{12}. Shown are the corresponding side-pairings transformations.

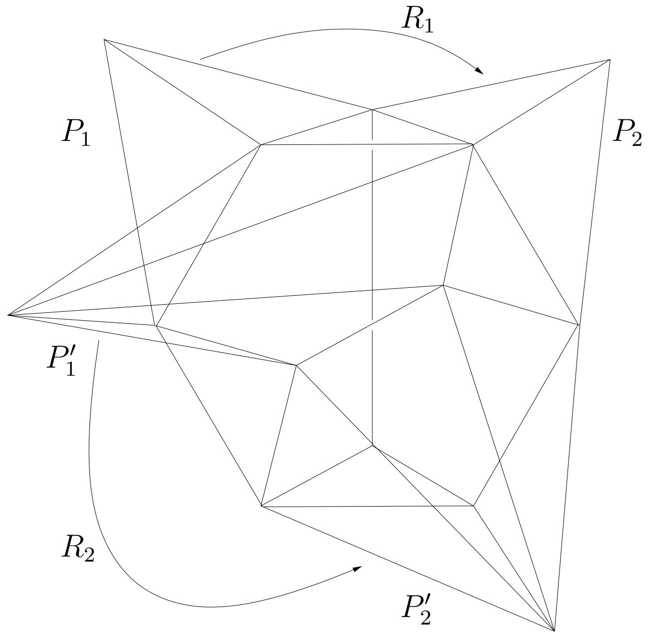

Figure 7: The 4 pentagonal pyramids in the boundary of Π and their side-pairing tranformations. Again, they are defined as cones to the common vertex p_{12}

T_1 based on τ_{11}.
Recall that $\tau_{11} = (t_{23}, s_{31}, \tilde{s}_{21})$ is $\mathbb{C}$-planar. Now when we add the point p_{12}, we obtain a special configuration:

Lemma 3.1 *The triangles $\tau_{12} = (t_{23}, s_{31}, p_{12})$ and $\tau_{13} = (t_{23}, \tilde{s}_{21}, p_{12})$ are $\mathbb{R}$-planar.*

Proof. This can be seen by computing the two Hermitian triple products. Another proof is obtained by observing that the complex geodesics containing $[t_{23}, s_{31}]$ and $[t_{23}, p_{12}]$ respectively, are orthogonal. Indeed, by construction, the first one is a slice of B_1 and the second is the complex spine of B_1. □

This shows that three faces of the tetrahedron are naturally reconstructed from its vertices; there remains some flexibility in the choice of the fourth face, and we have chosen the union of geodesics from p_{12} to the opposite edge (this ensures that this face is in common with the neighboring pentagonal pyramid). We can moreover see the following:

Lemma 3.2 *The tetrahedron T_1 is contained in a (unique) bisector.*

Proof. We need to find a bisector B such that the $\mathbb{R}$-planar triangles τ_{12} and τ_{13} are each in a meridian of B and such that the $\mathbb{C}$-planar triangle τ_{11} is in a slice. This is possible because the geodesic $(t_{23}p_{12})$ common to both $\mathbb{R}$-planes (which is the only possible spine) lives in a $\mathbb{C}$-plane orthogonal to the possible slice. □

3.4.2 Description of a pentagonal pyramid

We also have a priori two isometry classes of pentagonal pyramids, however they share the same structure and we only describe the pyramid P_1 based on the $\mathbb{R}$-planar pentagon π_1.
What happens now is that when we add the point p_{12}, we obtain five triangular 2-faces, one of which is $\mathbb{C}$-planar ($(t_{23}t_{32}p_{12})$ is contained in $Fix(R_1)$), the two adjacent faces $(t_{23}s_{31}p_{12})$ and $(t_{32}s_{12}p_{12})$ are $\mathbb{R}$-planar (they are in common with the tetahedra T_1 and T_2), and the two remaining faces are not geodesic. In particular:

Lemma 3.3 *The pentagonal pyramid P_1 is not contained in a bisector.*

Proof. Indeed three of its faces are $\mathbb{R}$-planar, intersecting in two distinct geodesics, whereas any three (or more) $\mathbb{R}$-planes contained in a bisector intersect in a common geodesic (the real spine). □

4 Topology and combinatorial structure of Π

The reader can skip this section if he assumes Proposition 4.1. We will now show how the combinatorial structure of Π ensures that its topology is reasonable, in the following sense:

Proposition 4.1 *Topologically, the boundary polyhedron $\partial\Pi$ is a sphere S^3 and the whole polyhedron Π is a ball B^4.*

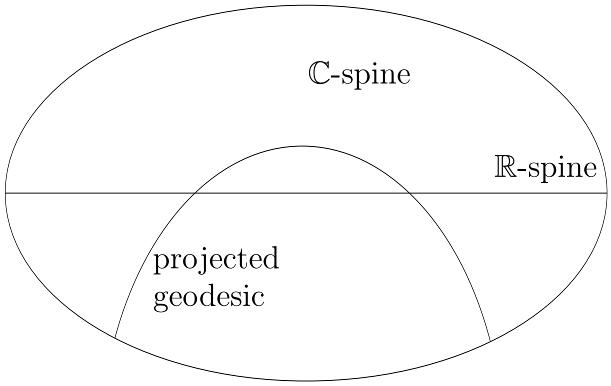

Figure 8: Generic intersection of a geodesic and a bisector

Proof. We show that $\partial\Pi$ is homeomorphic to S^3. The technical aspect is to show that the 3-faces as we have defined them intersect only where we expect them to, i.e. in common 2-faces or unions of 1-faces; this will be seen below and follows from the structure of the bisector faces and the special position of our cone point p_{12}. Assuming this, the fact that every 2-face belongs exactly to two 3-faces ensures that $\partial\Pi$ is a 3-manifold; in fact we have a realization of $\partial\Pi$ in S^3 by considering the core part $H \cup H'$ (a topological B^3) in $\mathbb{R}^3$ and setting the point p_{12} at infinity. $\partial\Pi$ is then the union of $H \cup H'$ with the cone from p_{12} over $\partial(H \cup H')$, which is the exterior of this ball; the verifications below ensure that this is an embedding. $\square$

We now want to check that the different 3-faces that we have defined intersect pairwise as expected (in 2-faces or unions of 1-faces), that is, that there is no unwanted extra intersection. A real difficulty resides in the fact that bisectors are not geodesically convex and that, more precisely, the generic intersection between a geodesic and a bisector is empty or a pair of points. This is a problem for us as we have defined our polyhedron as a geodesic cone over certain objects living in bisectors. For instance, it is possible that a geodesic between p_{12} and a point $q \in H$ meets H' before reaching q. We will see that this does not happen, the key point being that p_{12} is on the complex spines of both B_1 and B_1'.

Lemma 4.1 *Let C be a complex line and π_C be the orthogonal projection onto it. If γ is a geodesic intersecting C then $\pi_C(\gamma)$ is a geodesic in C.*

Note that this is not true in general, $\pi_C(\gamma)$ being an arc of Euclidean circle (see Figure 8).

Proof. Normalize the coordinates in the ball model so that $C = \{(z_1, 0) \in \mathbf{B}^2_{\mathbb{C}}\}$ and $C \cap \gamma = \{(0,0)\}$. Then the projection is simply $(z_1, z_2) \mapsto (z_1, 0)$ and the result is obvious knowing that the geodesics through the origin are the Euclidean segments. $\square$

We apply this simple fact to the context of bisectors. Recall the slice decomposition of a bisector: if B is a bisector with (real) spine g and complex spine C, and if as above π_C is the orthogonal projection onto C, then $B = \pi_C^{-1}(g)$ where the fibers $\pi_C^{-1}(\{p\})$ for $p \in g$ are the slices of B. The above lemma implies:

Lemma 4.2 *Let B be a bisector with (real) spine g and complex spine C, and let $p \in C$. Then the geodesics through p:*

- *intersect B in $\{p\}$ or are contained in B if $p \in g$*
- *intersect B in at most a point if $p \notin g$.*

Proof. The first part comes from the fact that the (real) spine is contained in all meridians. For the second part, the preceding lemma shows that if γ is a geodesic through p, then $\pi_C(\gamma)$ intersects g in at most a point q. Then $B \cap \gamma$ is contained in the slice $\pi_C^{-1}(\{q\})$. The slice being totally geodesic, this shows that $B \cap \gamma$ contains only one point. □

We are now ready to analyze the different intersections of 3-faces.

4.0.3 Intersection of the pentagonal pyramids with H and H'

There are two types of intersection between a pentagonal pyramid and a core face H or H', as follows:

Proposition 4.2

- *P_1 intersects H in the pentagon π_1*
- *P_1 intersects H' in two geodesic segments, $[\tilde{s}_{32}s_{31}]$ and $[\tilde{s}_{32}s_{12}]$.*

Proof. We prove the stronger statement that $P_1 \cap B_1 = \pi_1$ and $P_1 \cap B_1' = [\tilde{s}_{32}s_{31}] \cup [\tilde{s}_{32}s_{12}]$, by projecting to the $\mathbb{C}$-spine of the appropriate bisector and using the above lemma. Let $\pi_{C_1}, \pi_{C_1'}$ denote the orthogonal projection to the $\mathbb{C}$-spine of B_1 (resp. B_1').

For the first point: since $\pi_1 \subset B_1$, $\pi_{C_1}(\pi_1)$ is contained in the (real) spine of B_1, so that the preceding lemma implies that each geodesic from p_{12} to a point q of π_1 intersects B_1 only in q.

It remains to see how P_1 intersects H'. We start off by showing that the pentagon π_1 is entirely contained in the half-space bounded by B_1' and containing p_{12}. Recall that π_1 is contained in the $\mathbb{R}$-plane L_τ (see Proposition 2.10). Now L_τ has singular intersection with B_1', consisting in the two orthogonal geodesics $(\tilde{s}_{32}s_{31})$ and $(\tilde{s}_{32}s_{12})$ which separate L_τ into 4 regions as in Figure 9 (where $+$ and $-$ indicate the half-spaces bounded by B_1'). Thus π_1 (which is convex) is entirely contained in one of these half-spaces, which contains the vertices t_{23} and t_{32}. Now we can check, using two points from which B_1' is equidistant, such as p_{12} and p_{23}, that t_{23} and t_{32} are on the same side of B_1' as the point p_{12}. (Figure 10 illustrates the difference $cosh(\rho(t_{23}, p_{23})) - cosh(\rho(t_{23}, p_{12}))$ as a function of the phase shift t, the point being that it remains positive for $|t| < \frac{1}{2} - \frac{1}{p}$). We can then conclude, by projecting to the $\mathbb{C}$-spine of B_1' and using the lemma, that the whole cone P_1 is on the same side of B_1' as p_{12}, which implies that P_1 and B_1' have the desired intersection which is the pair of edges $[\tilde{s}_{32}s_{31}]$ and $[\tilde{s}_{32}s_{12}]$.

□

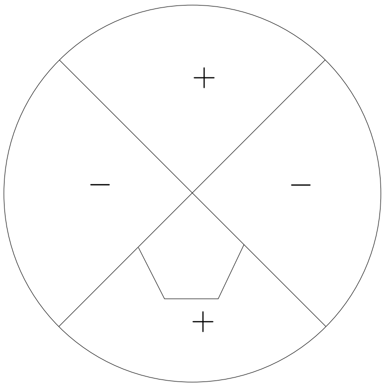

Figure 9: The trace of B_1' on the $\mathbb{R}$-plane L_τ

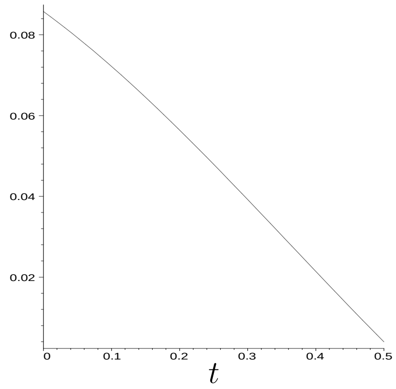

Figure 10: t_{23} is on the same side of B_1' as p_{12}

The same argument applies to the other pentagonal pyramids, knowing that t_{13} and t_{31} are on the same side of B_1 as the point p_{12}.

4.0.4 Intersection of the tetrahedra with H and H'

These intersections are exactly as above, replacing the pentagons with triangles. We have in this case:

Proposition 4.3 • *T_1 intersects H in the triangle τ_{11}*

• *T_1 intersects H' in the geodesic segment $[\tilde{s}_{21}s_{31}]$.*

4.0.5 Intersection of two cone faces

The intersection of two faces which are unions of geodesics from p_{12} is not much of a problem.

Lemma 4.3 *If α, β are subsets of $\partial(H \cup H')$, then:*

$$Cone(\alpha) \cap Cone(\beta) = Cone(\alpha \cap \beta)$$

Proof. It is obvious that: $Cone(\alpha \cap \beta) \subset Cone(\alpha) \cap Cone(\beta)$. That there is no extra intersection follows from what we have seen on the other faces. $\square$

4.0.6 Intersection of the two core faces H and H'

This is the easiest case because we have defined the 2-face η so that: $H \cap H' = \eta$. Note that H (resp. H') lies entirely on one side of bisector B_1' (resp. B_1), which is the same side as p_{12} as we have seen by testing the vertices.

5 Using Poincaré's polyhedron theorem

In this section we review Poincaré's polyhedron theorem. We will follow the general formulation of the theorem given in Mostow [M1], section 6 pg. 197, and we refer to it for a proof (see also [FP, Mas]). We define a polyhedron as a cellular space homeomorphic to a compact polytope. In particular, each codimension two cell is contained in exactly two codimension one cells. Its realization as a cell complex in a manifold X is also referred to as a polyhedron. We will say a polyhedron is smooth if its faces are smooth.

Definition 5.1 *A Poincaré polyhedron is a smooth polyhedron D in X with codimension one faces T_i such that*

1. *The codimension one faces are paired by a set Δ of homeomorphisms of X which respect the cell structure (the side pairing transformations). We assume that if $\gamma \in \Delta$ then $\gamma^{-1} \in \Delta$.*
2. *For every $\gamma_{ij} \in \Delta$ such that $T_i = \gamma_{ij} T_j$ then $\gamma_{ij} D \cap D = T_i$.*

Remark 5.1 If $T_i = T_j$, that is if a side pairing maps one side to itself then we impose, moreover, that γ_{ij} be of order two and call it a reflection. We refer to the relation $\gamma_{ij}^2 = 1$ as a reflection relation.

Let T_1 be an $(n-1)$-face and F_1 be an $(n-2)$-face contained in T_1. Let T_1' be the other $(n-1)$-face containing F_1. Let T_2 be the $(n-1)$-face paired to T_1' by $g_1 \in \Delta$ and $F_2 = g_1(F_1)$. Again, there exists only one $(n-1)$-face containing F_2 which we call T_2'. We define recursively g_i and F_i, so that $g_{i-1} \circ \cdots \circ g_1(F_1) = F_i$.

Definition 5.2 (Cyclic) Cyclic *is the condition that for each pair (F_1, T_1)(an $(n-2)$-face contained in an $(n-1)$-face), there exists $r \geq 1$ such that, in the construction above, $g_r \circ \cdots g_1(T_1) = T_1$ and $g_r \circ \cdots g_1$ restricted to F_1 is the identity. Moreover, calling $g = g_r \circ \cdots \circ g_1$, there exists a positive integer m such that $g_1^{-1}(P) \cup (g_2 \circ g_1)^{-1}(P) \cup \cdots \cup g^{-1}(P) \cup (g_1 \circ g)^{-1}(P) \cup (g_2 \circ g_1 \circ g)^{-1}(P) \cup \cdots \cup (g^m)^{-1}(P)$ is a cover of a closed neighborhood of the interior of F_1 by polyhedra with disjoint interiors.*

The relation $g^m = (g_r \circ \cdots g_1)^m = Id$ is called a *cycle relation*.

Theorem 5.2 *Let D be a compact Poincaré polyhedron with side-pairing transformations $\Delta \subset Isom(H^2_{\mathbb{C}})$ in $H^2_{\mathbb{C}}$ satisfying condition* **Cyclic**. *Let Γ be the group generated by Δ. Then Γ is a discrete subgroup of $Isom(H^2_{\mathbb{C}})$ and D a fundamental domain. A presentation is given by*

$$\Gamma = \langle \Delta \mid \textit{cycle relations, reflection relations} \rangle$$

5.1 Side-pairings

The side-pairings of our polyhedron Π are, writing $R_2 = JR_1J^{-1}$:

$$H \xrightarrow{J} H'$$

$$P_1 \xrightarrow{R_1} P_2 \qquad\qquad P_1' \xrightarrow{R_2} P_2'$$

$$T_1 \xrightarrow{(R_2R_1)^{-1}} T_1' \qquad\qquad T_2 \xrightarrow{R_1R_2} T_2'$$

5.2 Cycles and orbits of faces

We now write the cycles of 2-faces induced by the side-pairings, according to type of 2-face.

- The hexagon cycle:

$$\eta \xrightarrow{J} \eta \xrightarrow{J} \eta \xrightarrow{J} \eta$$

- The pentagon cycle:

$$\pi_1 \xrightarrow{R_1} \pi_2 \xrightarrow{J} \pi_2' \xrightarrow{R_2^{-1}} \pi_1' \xrightarrow{J^{-1}} \pi_1$$

- The $\mathbb{C}$-planar triangle cycles:

$$\tau_{11} \xrightarrow{(R_2R_1)^{-1}} \tau_{11}' \xrightarrow{J^{-1}} \tau_{11}$$

$$\tau_{21} \xrightarrow{R_1R_2} \tau_{21}' \xrightarrow{J^{-1}} \tau_{21}$$

$$\tau_{c1} \xrightarrow{R_1} \tau_{c1}$$

$$\tau_{c2} \xrightarrow{R_2} \tau_{c2}$$

- The $\mathbb{R}$-planar triangle cycles:

$$\tau_{12} \xrightarrow{R_1} \tau_{13} \xrightarrow{(R_2R_1)^{-1}} \tau'_{13} \xrightarrow{R_2^{-1}} \tau'_{12} \xrightarrow{R_2R_1} \tau_{12}$$

$$\tau_{22} \xrightarrow{R_1} \tau_{23} \xrightarrow{R_1R_2} \tau'_{23} \xrightarrow{R_2^{-1}} \tau'_{22} \xrightarrow{(R_1R_2)^{-1}} \tau_{22}$$

- The generic triangle cycles:

$$\tau_{14} \xrightarrow{(R_2R_1)^{-1}} \tau'_{14} \xrightarrow{R_1} \tau_{g2} \xrightarrow{R_2} \tau_{14}$$

$$\tau_{24} \xrightarrow{R_1R_2} \tau'_{24} \xrightarrow{R_1^{-1}} \tau_{g1} \xrightarrow{R_2^{-1}} \tau_{24}$$

5.3 Verifying the tessellation conditions

5.3.1 First step: the side-pairings send Π off itself

We show in this section that each side-pairing g of Π satisfies:

$$\overset{\circ}{\Pi} \cap g(\overset{\circ}{\Pi}) = \emptyset$$

This is more easily seen in the case where the faces corresponding to the side-pairing live in a bisector, because the bisector in question separates Π and its image, hence the intersection of these polyhedra has dimension at most 3, and their interiors are disjoint. We now verify this claim.

- Side-pairing J

  J maps H to H', which lives in the bisector B'_1. We have:

  Proposition 5.1 *B'_1 separates Π and $J(\Pi)$.*

  Proof. We first see this for the core parts $H \cup H'$ and $J(H \cup H') = H' \cup H''$. Now H' is in B'_1 so we only need to check that H is on one side of B'_1 and H'' on the other. We already know that H is on the same side of B'_1 as p_{12} (see section 4.0.6), and the second part follows, knowing that the $\mathbb{R}$-reflection σ_{13} (in the meridian L_{13} of B'_1) exchanges H and H'', as can be checked on the vertices.

  The cone parts are then easily seen to be on the appropriate sides of B'_1, because the cone points p_{12} and $p_{23} = J(p_{12})$ are in the $\mathbb{C}$-spine of B'_1, each on the same side as the base of its cone. □

- Side-pairings R_1R_2 and R_2R_1:

  We treat the case of R_1R_2, the other being completely analogous. R_1R_2 maps T_2 to T_2' which is contained in the bisector $B_{T_2'}$, having as real spine the geodesic $(t_{13}p_{12})$. We have:

  Proposition 5.2 *$B_{T_2'}$ separates Π and $R_1R_2(\Pi)$.*

  Proof. It suffices to show that Π is entirely on one side of $B_{T_2'}$. Indeed, Π is then analogously entirely on one side of B_{T_2}, so that by the side-pairing R_1R_2, $R_1R_2(\Pi)$ is entirely on one side of $B_{T_2'} = R_1R_2(B_{T_2})$. We then check one point in each polyhedron to see that they are indeed on opposite sides.

  The fact that Π is entirely on one side of $B_{T_2'}$ can be seen by projecting to the $\mathbb{C}$-spine of $B_{T_2'}$ (the mirror of R_2), which contains the points p_{12}, t_{13}, t_{31}.

  - Position of H': H' lives in the bisector B_1', which has the same $\mathbb{C}$-spine as $B_{T_2'}$; its projection is thus contained in the geodesic $(t_{13}t_{31})$ (the real spine of B_1'), and in light of the foliation of H' by complex triangles it is in fact inside the segment $[t_{13}t_{31}]$.
  - Position of H: Recall that the 2-skeleton of H consists in η, π_1, π_2, τ_{11} and τ_{21}.

    η is also in H' so it projects in the segment $[t_{13}t_{31}]$. For the pentagons we need the following lemma:

    Lemma 5.1 *The four points p_{12}, $\tilde{s}_{21}$, t_{13}, t_{23} (respectively, p_{12}, s_{12}, t_{31}, t_{32}) lie in a common $\mathbb{R}$-plane.*

    Proof. Indeed, as we have seen earlier, the triples $(p_{12}, \tilde{s}_{21}, t_{13})$, $(p_{12}, \tilde{s}_{21}, t_{23})$ and $(\tilde{s}_{21}, t_{13}, t_{23})$ each lie in an $\mathbb{R}$-plane because the pairs of geodesics $(p_{12}t_{13})$ and $(\tilde{s}_{21}t_{13})$, $(p_{12}t_{23})$ and $(\tilde{s}_{21}t_{23})$, $(\tilde{s}_{21}t_{13})$ and $(\tilde{s}_{21}t_{23})$ lie in pairwise orthogonal complex lines. Thus we have a tetrahedron of which 3 faces are $\mathbb{R}$-planar: by Proposition 2.9 this is possible only if the four points lie in the same $\mathbb{R}$-plane. □

    We can now analyze the position of π_2. As we have just seen, the geodesic $(\tilde{s}_{21}t_{23})$ is contained in (a meridian of) $B_{T_2'}$, which also contains $(\tilde{s}_{21}s_{23})$ in a complex slice. Thus the intersection of the $\mathbb{R}$-plane containing π_2 with $B_{T_2'}$ is exactly a pair of geodesics, which are two sides of π_2, so that π_2 lies entirely on one side of $B_{T_2'}$, as in Figure 9.

    We now use the other quadruple of points of the lemma: these lie on an $\mathbb{R}$- plane which is for instance a meridian of the bisector $B_{T_1'}$ having $(p_{12}t_{31})$ as real spine (and having the same $\mathbb{C}$-spine as $B_{T_2'}$). Thus the entire quadrilateral projects into the segment $[p_{12}t_{31}]$. We now know that the 1-skeleton of H projects to the appropriate side of $B_{T_2'}$, except maybe for the edge $[s_{31}t_{23}]$. This is the third side of the $\mathbb{C}$-planar triangle τ_{11}, whose two other sides, $[\tilde{s}_{21}t_{23}]$ and $(\tilde{s}_{21}s_{31})$, project as we have seen into the segments $[t_{13}p_{12}]$ and $[t_{13}t_{31}]$ respectively (see Figure 11). This gives us sufficient control over the third side. Indeed, the projection restricted to a complex face is holomorphic, thus an open and angle-preserving map. This rules out the possibility that the image of the edge $[s_{31}t_{23}]$ (which is an arc of hypercycle in the $\mathbb{C}$-spine of

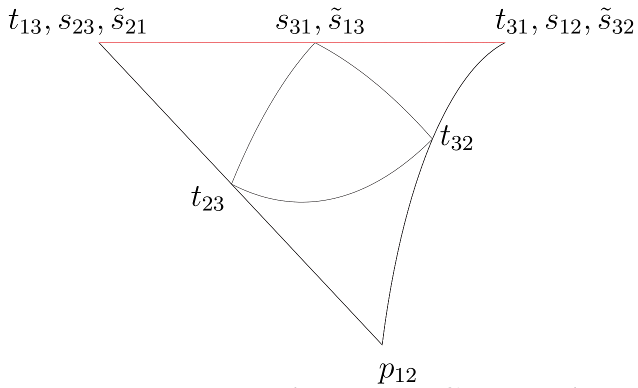

Figure 11: Projection of H to the $\mathbb{C}$-spine of $B_{T_2'}$

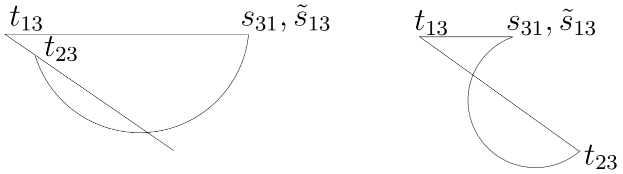

Figure 12: Non-admissible projections of a complex triangle

$B_{T_2'}$) pass through the real spine ($t_{13}p_{12}$) (see Figure 12; the first case is ruled out by "angle-preserving" and the second by "open"). We then conclude by saying that the image of H is bounded by the image of its boundary, using for instance the foliation of H by complex triangles.

– Position of the cone faces: As earlier the geodesics through p_{12} project to geodesics because p_{12} is in the complex line onto which we are projecting; moreover p_{12} is in the real spine of $B_{T_2'}$, so that the cone on an object is entirely on the same side of $B_{T_2'}$ as that object.

□

- Side-pairings R_1 and R_2:

  This is the most delicate case because Π and its image cannot be separated by a bisector (or else this bisector would contain one of the pentagonal pyramids, which we have seen to be impossible).

  To prove that $R_1(\Pi)$ and Π have disjoint interiors, a possible approach would be to show that Π is contained in a fundamental domain for R_1 (as suggested to us by the referee). In fact R_1 acts on complex lines orthogonal to its mirror as a rotation. Therefore, the choice of a wedge (of angle $2\pi/p$) in each of these lines defines a fundamental domain for R_1. Unfortunately, there does not seem to be a simple global choice of such wedges.

  Instead we have to consider separately the core faces and the cone faces, and use the fact that if the interiors of the polyhedra were to meet, then so would the interiors of some of their 3-faces.

Proposition 5.3

$$\mathring{\Pi} \cap R_1(\mathring{\Pi}) = \emptyset$$

Proof. We follow the lines given above, first separating the core faces (H and H', $R_1(H)$ and $R_1(H')$). The only obvious intersection between these faces is that of H and $R_1(H)$ (namely P_2), which live in the same bisector B_1.

We first prove the following

Lemma 5.2 *There exists a bisector B_{R_1} which separates $H \cup H'$ and $R_1(H \cup H')$. In particular, these two objects have disjoint interiors.*

Observe that the four faces in question all have the edges $[\tilde{s}_{13}s_{23}]$ and $[s_{23}\tilde{s}_{21}]$ in common, so that a suitable bisector must contain these edges. In fact our bisector will contain the whole $\mathbb{R}$-plane $R_1(L_\tau)$ as a meridian.

The most natural idea is to use one of the complex slices of B_1 as a $\mathbb{C}$-spine for our bisector (the $\mathbb{C}$-plane onto which we will project). For practical reasons we use the slice containing s_{23} and $\tilde{s}_{32}$ (this is the slice containing the largest section of H). We thus define B_{R_1} by its real spine which is the geodesic joining s_{23} and its projection to the vertical axis $(t_{23}t_{32})$. The first thing to say is:

Lemma 5.3 *The bisectors B_1 and B_{R_1} intersect only along the common meridian $R_1(L_\tau)$.*

Proof. It is clear that B_1 and B_{R_1} share this meridian, because it contains both real spines. One can then invoke [Go] pg. 174, or use Proposition 2.9 on $\mathbb{R}$-planar tetrahedra to conclude. $\square$

This shows that H is entirely on one side of B_{R_1} (and $R_1(H)$ on the other). Consider now H'; we examine each 2-face separately.

- The most obvious is the hexagon η, which also belongs to H.
- The $\mathbb{C}$-planar triangle τ'_{21} has an edge, $[s_{23}\tilde{s}_{21}]$, which is in B_{R_1}. That geodesic can be the only intersection between B_{R_1} and the $\mathbb{C}$-plane containing τ'_{21}, so that τ'_{21} is entirely on one side of B_{R_1}.
- The $\mathbb{R}$-planar pentagon π'_1 also has an edge which is in B_{R_1}, namely $[s_{23}\tilde{s}_{13}]$. Now this geodesic meets the $\mathbb{R}$-spine of B_{R_1}, in s_{23}, so that by Proposition 2.8 it can be the only intersection between the $\mathbb{R}$-plane $R_1(L_\tau)$ and B_{R_1}. Thus the whole pentagon is on one side of B_{R_1}.

So far, we know that the entire 1-skeleton of H' is on one side of B_{R_1}, except maybe for the edge $[\tilde{s}_{32}t_{31}]$. Now this edge meets the $\mathbb{C}$-spine of B_{R_1} (in $\tilde{s}_{32}$) so it projects to a geodesic and stays on the same side of B_{R_1} as its endpoints. Having the 1-skeleton, we extend the result to the 2-skeleton: the only non-obvious faces are a $\mathbb{C}$-planar triangle and an $\mathbb{R}$-planar pentagon of H', which are handled by Lemma 2.1. Finally, we get the corresponding result for all of H' by using the foliation of H' into $\mathbb{C}$-planar triangles.

Thus $H \cup H'$ is entirely on one side of B_{R_1}; the same arguments (replacing the $\mathbb{R}$-plane $R_1(L_\tau)$ by L_τ) prove that $H \cup H'$ is entirely on one side of $B_{R_1^{-1}}$ (the bisector analogous

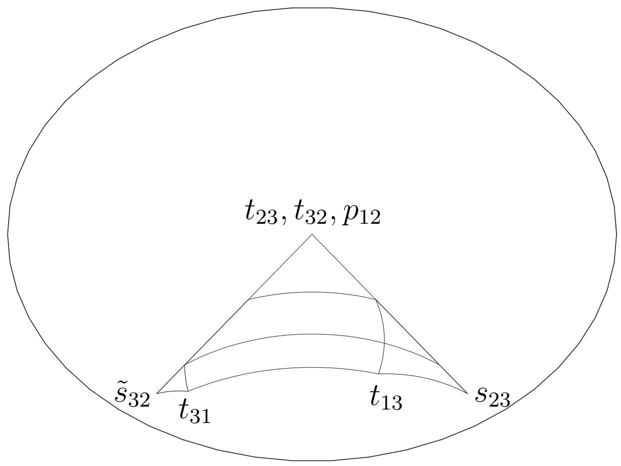

Figure 13: Projection of H and H' to the $\mathbb{C}$-spine of B_{R_1}

to B_{R_1}, but containing L_τ), so that in fact $H \cup H'$ is entirely in the "wedge" of angle $\frac{2\pi}{p}$ between B_{R_1} and $B_{R_1^{-1}}$ (see Figure 13).

We conclude by noting that R_1 rotates the $\mathbb{C}$-spine of B_{R_1} by an angle $\frac{2\pi}{p}$ (around the point image of t_{23}, t_{32}, p_{12}), sending the wedge off itself. $\square$

To conclude the proof of the proposition, it remains to see what happens with the cone faces: we have already seen, when describing the self-intersection of Π, that the cones from p_{12} on H and H' have no other intersection than the cone on their intersection. There remain three intersecting pairs to analyze:

Lemma 5.4 *1. $Cone(H') \cap Cone(R_1(H)) = Cone(H' \cap R_1(H))$*

2. $Cone(H) \cap Cone(R_1(H')) = Cone(H \cap R_1(H'))$

Proof. We start with the first item. We project the cones to both complex spines of B_1 and B_1'. If a geodesic containing p_{12} is in the intersection of the cones it projects onto a geodesic under both projections by Lemma 4.1. Such a geodesic will meet either H' or $R_1(H)$ first. The lemma is proven if we show that the geodesic meets H' and $R_1(H)$ at the same time. To see this, recall from section 4.0.3 that the projection of H' in the complex spine of B_1 is on the same side as p_{12} with respect to the real spine (which contains the projection of $R_1(H)$).

This shows that the geodesic meets H' first. Projecting to the complex spine of B_1' shows analogously that the same geodesic meets $R_1(H)$ first. Indeed, $R_1(H)$ is contained in B_1, on the same side of the surface S_η as H as can be seen slice by slice (if C is a slice of B_1, $S_\eta \cap C$ is a hypercycle, i.e. an arc of a Euclidean circle meeting twice the boundary circle, bounding $C \cap H$ and $C \cap R_1(H)$ is on the same side of this arc as that of $C \cap H$, see Figure 14); thus $R_1(H)$ is on the same side of B_1' as H and p_{12}.

The second item is proved analogously, noting that in a slice C of B_1, $C \cap H$ is on the same side of the hypercycle $C \cap R_1(S_\eta)$ as $C \cap R_1(H)$. $\square$

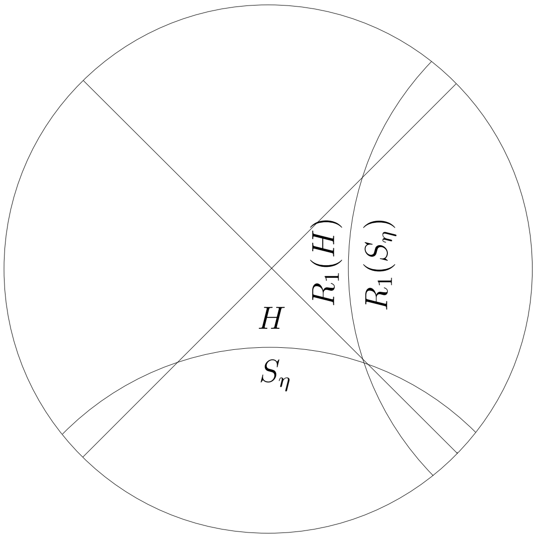

Figure 14: View of a complex slice of B_1 (for $p = 4$)

Lemma 5.5 $Cone(H') \cap Cone(R_1(H')) = Cone(H' \cap R_1(H'))$

Proof. We project the cones on the complex spines of B_1' (which contains H') and $R_1(B_1')$ (which contains $R_1(H')$). Since p_{12} is in both complex spines, as in the previous lemma, the projections of the cones are cones over the projection by Lemma 4.1. The same argument as above will hold if we show that each projection is on the same side as p_{12} with respect to the corresponding real spine; we will refer to that side as the *good* side.

To show this, let us first consider the projection of $R_1(H')$ on the complex spine of B_1'. We check that the vertices of $R_1(H')$ are all in the same side of B_1' as p_{12}. That gives a hint that the whole 3-face $R_1(H')$ is in the good side. More precisely, we divide the proof in several steps:

1. We check numerically that $R_1(t_{13})$ and $R_1(t_{31})$ are in the good side of B_1'.
2. From the knowledge of $S_\eta = B_1 \cap B_1'$, which is a union of hypercycles, one in each slice of B_1, we obtain that $R_1(\eta)$ intersects S_η in precisely two geodesic segments $[\tilde{s}_{21}, s_{23}]$ and $[s_{23}, \tilde{s}_{13}]$ and, moreover, is contained in the good side of B_1'.
3. As the intersection of $R_1(\tau_{11}')$ (a slice of $R_1(H')$) with B_1' is a hypercycle and contains the geodesic segment $[s_{23}, \tilde{s}_{13}]$, we conclude that $R_1(\tau_{11}')$ is in the good side.
4. We have to check that the pentagonal faces $R_1(\pi_i')$, $i = 1, 2$, project on the good side. Observe that the Lagrangian pentagon $R_1(\pi_2')$ has a geodesic in common with the bisector B_1', namely $[\tilde{s}_{21}, s_{23}]$. Now the intersection of the whole Lagrangian with the bisector could contain at most one more geodesic, orthogonal to the first (see Proposition 2.8). However, if such a second geodesic existed and met the pentagon $R_1(\pi_2')$, the vertices of $R_1(\pi_2')$ would lie on both sides of this geodesic (because the pentagon has only right angles) and thus on both sides of B_1'. This is impossible since we have verified that all points are on the same side of B_1'. We conclude that the whole pentagon is on the good side.

Concerning the other pentagon $R_1(\pi_1')$, the same argument does not apply (because a priori it has no intersection with B_1'), and it remains to check that one of its edges is in the good side, namely the edge $[R_1(t_{13}), R_1(s_{23})]$. This is done in the next item.

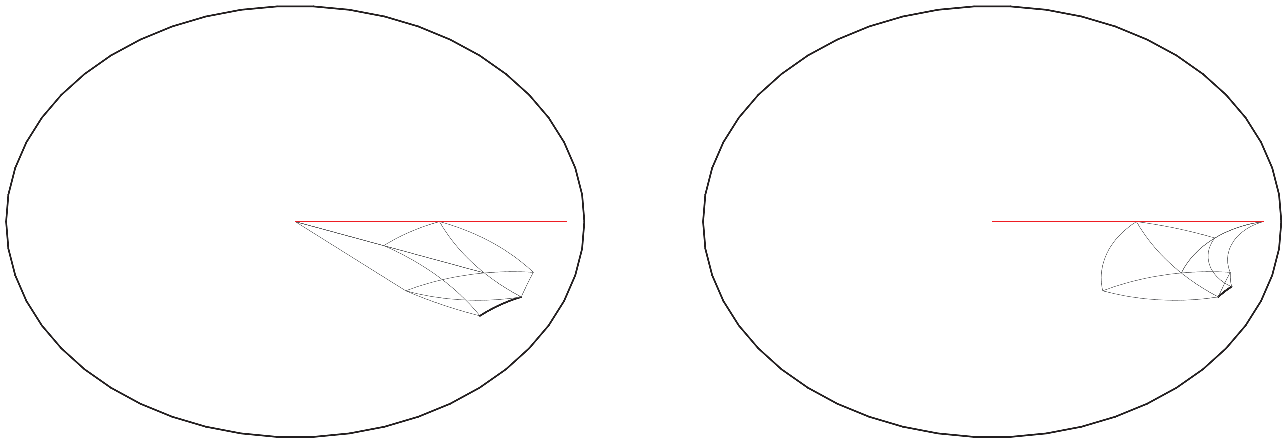

(a) $Cone(R_1(H'))$ projected onto $e_2^\perp$ (b) $Cone(H')$ projected onto $R_1(e_2^\perp)$

Figure 15: The straight line segments represent the spine of the relevant bisector, which we need to separate H' and $R_1(H')$. The thick segment is the only one that we need to check numerically. The pictures are drawn for $p = 3$ and $t = 1/18$.

5. We need to prove the following statement, which seems quite obvious on Figure 15: the geodesic segment between $R_1(t_{13})$ and $R_1(s_{23})$ does not intersect the bisector B_1'. Computer investigation shows that a stronger statement is true, namely that the entire geodesic (and not only the segment) does not intersect the relevant bisector. We shall explain how this can be done for the first case only, the second one being completely analogous.
   Let γ be the geodesic segment between $p = R_1 t_{13}$ and $q = R_1 s_{23}$. We claim that it never intersects the bisector B_1' equidistant from p_{12} and p_{23}.
   We write $\gamma(x) = (1-x)p + xq/\langle q, p\rangle = v + xw$ (note the geodesic is not parameterized with constant speed, so the parameter x should range through some interval, whose endpoints are irrelevant to our computation).
   Any possible intersection of γ with B_1' would be found by solving the equation
$$|\langle v + xw, p_{12}\rangle| = |\langle v + xw, p_{23}\rangle| \tag{5.1}$$
   Using the linearity of the Hermitian product and squaring both sides of the equation, we can rewrite it in the form of a quadratic equation
$$ax^2 + bx + c = 0 \tag{5.2}$$
   where
$$a = |\langle w, p_{12}\rangle|^2 - |\langle w, p_{23}\rangle|^2 \tag{5.3}$$
$$b = 2\mathfrak{Re}\left(\langle v, p_{12}\rangle\langle p_{12}, w\rangle - \langle v, p_{23}\rangle\langle p_{23}, w\rangle\right) \tag{5.4}$$
$$c = |\langle v, p_{12}\rangle|^2 - |\langle v, p_{23}\rangle|^2 \tag{5.5}$$

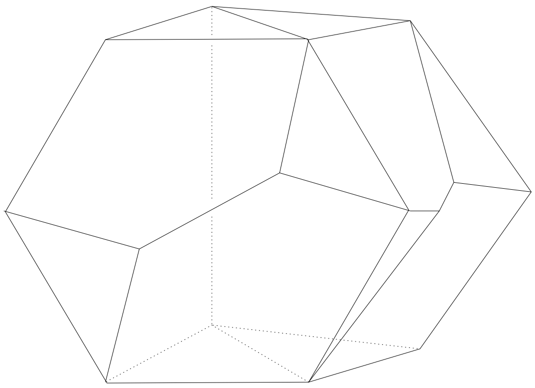

Figure 16: The 3-faces H' and $R_1(H')$ and H and $R_1(H)$. Note that H and $R_1(H)$ are contained in the bisector B_1.

It can easily be checked that the discriminant of this quadratic equation is negative for small phase shift. The values of $\Delta = b^2 - 4ac$ for the values of t corresponding to discrete groups with $p = 3$ are given in the following table:

t	Δ
0	$-0.2369\ldots$
1/30	$-0.2465\ldots$
1/18	$-0.2472\ldots$
5/42	$-0.2236\ldots$

6. The projection of the face $R_1(H')$ in the complex spine of B_1' is bounded by the image of its 2-skeleton because $R_1(H')$ is foliated by triangles in slices and the image by the projection (a holomorphic map) of each triangle is a triangle in the complex spine of B_1'. In fact it is also bounded by the projection of the 1-skeleton by Lemma 2.1. Using the items above we then conclude the proof that the projection of the face $R_1(H')$ in the complex spine of B_1' is in the good side.

The same argument shows that H' is in the good side of $R_1(B_1')$. In particular a key step is to show that the geodesic segment between t_{31} and $\tilde{s}_{32}$ does not intersect the bisector $R_1(B_1')$ (see again Figure 15).

To conclude the proof of the lemma we show as above, by projecting to both $\mathbb{C}$-spines, that the intersection on the cones over the bases has to contain a point of the intersection of the bases. □

The proposition follows from the three main lemmas. □

5.3.2 Second step: further along the cycles

In this section we verify condition **Cyclic** of the Poincaré theorem. Recall that for a cycle of codimension-2-faces ϕ_i:

$$\phi_1 \xrightarrow{g_1} \phi_2 \xrightarrow{g_2} \dots \phi_k \xrightarrow{g_k} \phi_1$$

the cycle transformation $g_k \circ g_{k-1} \dots \circ g_1$ has a certain finite order m (this is one of the hypotheses we have to check; the side-pairings g_i are explicit in matrix form which allows us to find m). We will call k the *length* of the cycle, and $m \cdot k$ its *total length.* Condition **Cyclic** ensures that the $m \cdot k$ images of Π:

$$g_1^{-1}(\Pi), (g_2 \circ g_1)^{-1}(\Pi), \dots, ((g_k \circ g_{k-1} \dots \circ g_1)^m)^{-1}(\Pi) = \Pi$$

tile a neighborhood of the face ϕ_1. In fact, each of these polyhedra shares a codimension-1-face with its two closest neighbors, so that we only need to check that all of these polyhedra have pairwise disjoint interiors.

We have shown in the preceding section that this is true for all pairs of adjacent polyhedra (those differing by a side-pairing). This settles the case of all cycles of maximum total length 3; for greater total length we must check that Π and its non-adjacent images have disjoint interiors. We will start with the 3 cycles of total length 4, where we only need to compare Π with its "diagonal" image (see diagrams below). The cycles of total length 4 are:

- the pentagon cycle:

$$\pi_1 \xrightarrow{R_1} \pi_2 \xrightarrow{J} \pi_2' \xrightarrow{R_2^{-1}} \pi_1' \xrightarrow{J^{-1}} \pi_1$$

A schematic picture of the tiling of a neighborhood of the 2-face π_1 (represented by the central vertex) is:

$J^{-1}(\Pi) =$ $R_1^{-1}.J^{-1}.R_2(\Pi)$	Π
$J^{-1}.R_2^{-1}(\Pi)$ $= R_1^{-1}.J^{-1}(\Pi)$	$R_1^{-1}(\Pi)$

The fact that Π and its "diagonal" image $J^{-1}.R_2^{-1}(\Pi) = R_1^{-1}.J^{-1}(\Pi)$ have disjoint interiors follows easily from what we have already seen. Indeed, we know that the bisector B_1 separates Π and $J^{-1}(\Pi)$. Now R_1 fixes pointwise the $\mathbb{C}$-spine of B_1 (which is its mirror) and commutes with the orthogonal projection onto it, so that it preserves each of the half-spaces bounded by B_1.

Thus, applying R_1^{-1} to $J^{-1}(\Pi)$, we see that B_1 separates Π from $R_1^{-1}.J^{-1}(\Pi)$.

- the $\mathbb{R}$-planar triangle cycles:

$$\tau_{12} \xrightarrow{R_1} \tau_{13} \xrightarrow{(R_2R_1)^{-1}} \tau_{13}' \xrightarrow{R_2^{-1}} \tau_{12}' \xrightarrow{R_2R_1} \tau_{12}$$

$$\tau_{22} \xrightarrow{R_1} \tau_{23} \xrightarrow{R_1R_2} \tau_{23}' \xrightarrow{R_2^{-1}} \tau_{22}' \xrightarrow{(R_1R_2)^{-1}} \tau_{22}$$

A diagram for the first cycle is:

$$\begin{array}{c|c} R_2.R_1(\Pi) = & \Pi \\ R_1^{-1}.R_2.R_1.R_2(\Pi) & \\ \hline R_1^{-1}.R_2.R_1(\Pi) & \\ = R_2.R_1.R_2^{-1}(\Pi) & R_1^{-1}(\Pi) \end{array}$$

As above, we can easily separate Π and its diagonal image $R_1^{-1}.R_2.R_1(\Pi) = R_2.R_1.R_2^{-1}(\Pi)$, this time by the bisector B_{T_1}. Indeed, B_{T_1} separates Π and $R_2.R_1(\Pi)$, as we have already seen, and as above R_1 preserves the half-spaces bounded by B_{T_1} (whose $\mathbb{C}$-spine is again the mirror of R_1), so that B_{T_1} separates Π and $R_1^{-1}.R_2.R_1(\Pi)$.

The second cycle is analogous.

Now the only other cycles with total length greater than 3 are the $\mathbb{C}$-planar triangle cycles:

$$\tau_{11} \xrightarrow{(R_2R_1)^{-1}} \tau_{11}' \xrightarrow{J^{-1}} \tau_{11}$$

$$\tau_{21} \xrightarrow{R_1R_2} \tau_{21}' \xrightarrow{J^{-1}} \tau_{21}$$

on one hand, which has length 2 but arbitrarily large total length, and:

$$\tau_{c1} \xrightarrow{R_1} \tau_{c1}$$

$$\tau_{c2} \xrightarrow{R_2} \tau_{c2}$$

on the other, of length 1 and of total length p (in our cases, $p = 3, 4$ or 5).

- We start with the first pair of cycles. The cycle transformations are respectively $(R_2R_1J)^{-1}$ and $J^{-1}R_1R_2$; they both fix pointwise a $\mathbb{C}$-plane, namely the one containing the triangle τ_{11} (resp. τ_{21}). Computing the eigenvalues of these two elements tells us that they act on $\mathbb{C}$-planes orthogonal to their mirror by multiplication by $\overline{\eta}i\overline{\varphi}^3$ (resp. $-\eta i\overline{\varphi}^3$), corresponding to rotations of angle $\pi(\frac{1}{2}-\frac{1}{p}\pm t)$. If the group is discrete, these elliptic elements are to have finite order. In fact, imposing the angles to be of the form $\frac{2\pi}{k}$, $\frac{2\pi}{l}$ with $k, l \in \mathbb{Z}\cup\{\infty\}$ is sufficient to obtain the cyclic condition for these two cycles, and thus discreteness of our group. Precisely:

Proposition 5.4 – *If $k = (\frac{1}{4} - \frac{1}{2p} + \frac{t}{2})^{-1} \in \mathbb{Z}$, the polyhedra*

$$\Pi,\ R_2R_1(\Pi),\ R_2R_1J(\Pi),\ ...,\ (R_2R_1J)^k(\Pi),\ (R_2R_1J)^kR_2R_1(\Pi)$$

have disjoint interiors. In fact, two of these share a common 3-face if they are adjacent, or else they only have the 2-face τ_{11} in common.

– *Analogously, if $l = (\frac{1}{4} - \frac{1}{2p} - \frac{t}{2})^{-1} \in \mathbb{Z}$,the polyhedra*

$$\Pi,\ (R_1R_2)^{-1}(\Pi),\ (R_1R_2)^{-1}J(\Pi),\ ...,\ ((R_1R_2)^{-1}J)^l(\Pi),\ ((R_1R_2)^{-1}J)^l(R_1R_2)^{-1}(\Pi)$$

have disjoint interiors, and two of them share a common 3-face if they are adjacent, or else they only have the 2-face τ_{21} in common.

Proof. We have just seen that the elements $(R_2R_1J)^{-1}$ and $J^{-1}R_1R_2$ act on $\mathbb{C}$-planes orthogonal to their mirror by certain rotations, the two integral conditions saying that these are of angle $\frac{2\pi}{k}$ and $\frac{2\pi}{l}$. Now we know that the $\mathbb{C}$-plane containing the points t_{23}, t_{32}, p_{12} (which is the common spine of bisectors B_1, B_{T_1}, B_{T_2}) is orthogonal to the mirrors of $(R_2R_1J)^{-1}$ and $J^{-1}R_1R_2$, at points t_{23} and t_{32} respectively. We project to this $\mathbb{C}$-plane, which contains the geodesic triangle (t_{23}, t_{32}, p_{12}), each of the sides being the real spine of one of the bisectors B_1, B_{T_1}, B_{T_2}. We have shown that the polyhedron Π is entirely on one side of each of these bisectors, which means that its projection is entirely inside of the triangle (t_{23}, t_{32}, p_{12}). This proves the proposition. $\square$

Remark 5.3 There are finitely many values of t for which the two numbers $(\frac{1}{4}-\frac{1}{2p}\pm\frac{t}{2})^{-1}$ are integers, listed in the following table:

p	$\lvert t\rvert < \frac{1}{2}-\frac{1}{p}$	$\lvert t\rvert = \frac{1}{2}-\frac{1}{p}$	$\lvert t\rvert > \frac{1}{2}-\frac{1}{p}$
3	$0, \frac{1}{30}, \frac{1}{18}, \frac{5}{42}$	$\frac{1}{6}$	$\frac{7}{30}, \frac{1}{3}$
4	$0, \frac{1}{12}, \frac{3}{20}$	$\frac{1}{4}$	$\frac{5}{12}$
5	$\frac{1}{10}, \frac{1}{5}$		$\frac{11}{30}, \frac{7}{10}$

Remark 5.4 It follows from what we have done that the group generated by $A = (R_2R_1J)^{-1}$ and $B = J^{-1}R_1R_2$ is a $\mathbb{C}$-Fuchsian triangle goup, preserving the mirror of R_1. Indeed, one checks that the product AB acts on this complex geodesic as a rotation by an angle $2\pi/N$, where $N = \frac{2p}{6-p}$, fixing p_{12} (a geometric reason for this value can be found in [M1], p.243). In particular, a fundamental domain for its action is given by the union of the triangle τ_{c1} and its reflection about the geodesic $(t_{23}t_{32})$.

- Now consider the last cycles, where the cycle transformations are R_1 and R_2, of order $p = 3, 4$ or 5. For $p = 3$ there is nothing to add, but for $p = 4$ or 5 we must ensure that the non-adjacent polyhedra Π and $R_i^2(\Pi)$ have disjoint interiors. We do this by following the lines of the analogous verification for Π and $R_i(\Pi)$ (proof of proposition 5.3); in principle the two non-adjacent polyhedra are easier to separate because they have a smaller intersection, however we lose some control over this intersection. Rather, we handle this by using the computer to check the position of the 16 core edges (as opposed to just 1 previously).

  The core faces are easily separated using the bisector B_{R_1} which was introduced in the proof of proposition 5.3:

  Lemma 5.6 *For $p = 4$ and 5, B_{R_1} separates $H \cup H'$ and $R_1^2(H \cup H')$.*

  Proof. This follows from what we have seen: we know that $H \cup H'$ projects to the $\mathbb{C}$-spine of B_{R_1} inside a wedge of angle $\frac{2\pi}{p}$ (see Figure 13) whose images under R_1^k $(k = 0, ..., p-1)$ tile this $\mathbb{C}$-plane. $\square$

  As before, two of the three cases of intersections of cones are easily described (using arguments of elementary plane geometry on hypercycles). However the bases of the cones are now disjoint, so that the cones intersect only at the common apex p_{12}, as follows:

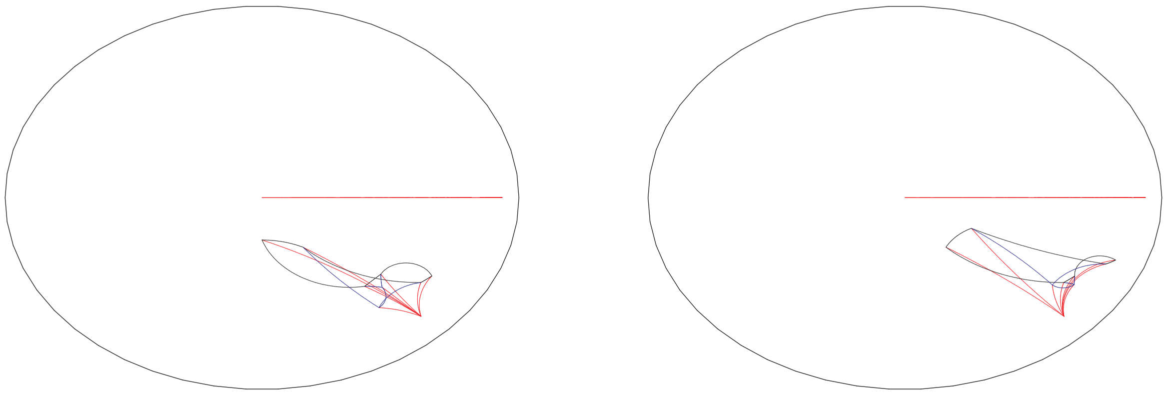

(a) $Cone(R_1^2(H'))$ projected onto $e_2^\perp$ (b) $Cone(H')$ projected onto $R_1^2(e_2)^\perp$

Figure 17: $Cone(H')$ and $Cone(R_1^2(H'))$ intersect only in the point p_{12}, as can be seen by projecting each one onto the complex spine of the other. The pictures are drawn for $p = 5$ and $t = 1/5$.

Lemma 5.7 *1.* $Cone(H') \cap Cone(R_1^2(H)) = \{p_{12}\}$

2. $Cone(H) \cap Cone(R_1^2(H')) = \{p_{12}\}$

The last case, which requires some numerical verifications, is the following:

Lemma 5.8 $Cone(H') \cap Cone(R_1^2(H')) = \{p_{12}\}$

Proof. As before, we consider simultaneously the projections to both complex spines of the bisectors containing the bases of the cones, namely B_1' and $R_1^2(B_1')$. Both complex spines contain the cone point p_{12}, so that the cones will behave well provided that the bases H' and $R_1^2(H')$ are on the appropriate side of these bisectors. Using the same arguments as earlier, we reduce this to a verification on the 1-skeleton of these 3-faces. It then remains to check the position of 16 edges for each face (32 in all), for every value of t where the integrality condition holds, listed in Remark 5.3. One way to do this is to plot the projection of these edges using a computer, as done in Figure 17. Note that the picture is fairly unambiguous in the sense that all edges are "very far" from the real spine, i.e. at a distance much larger than the implied precision. In principle, a detailed verification could also be written along the lines of part 5 of the proof of Lemma 5.5. □

6 Beyond the critical phase shift

In this section we describe the modification of the combinatorics of our polyhedron for $|t| \geq \frac{1}{2} - \frac{1}{p}$.

For small phase shift, the starting point of our construction is the hexagon η contained in the intersection of the two natural bisectors $B_1 = B(p_{12}, p_{13})$ and $B_1' = J(B_1)$. Recall that the sides of the hexagon are contained in the complex geodesics polar to the points v_{ijk} (see section 2.4).

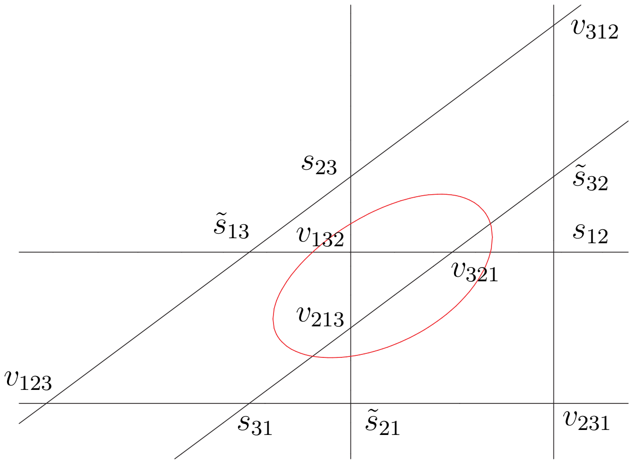

Figure 18: For large phase shift, some edges of the hexagon η are outside complex hyperbolic space. The corresponding face is a triangle, with vertices v_{132}, v_{213}, v_{321}, if $t > 0$.

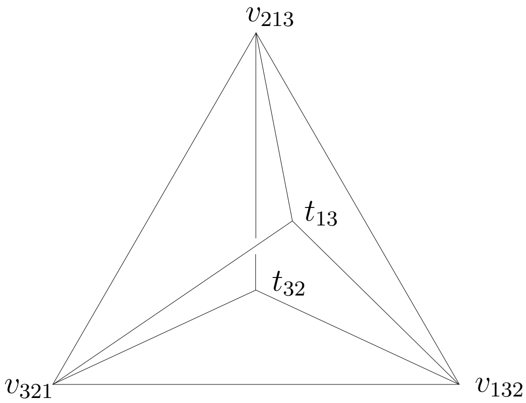

Figure 19: The core part $H \cup H'$ for large phase shift.

As already observed by Mostow, when $|t| = t_c := \frac{1}{2} - \frac{1}{p}$, the hexagon degenerates, three of its sides collapsing to points on the boundary (three of the v_{ijk}). After this critical value, the corresponding v_{ijk} are inside the ball (see Figure 18), and they replace their polar triangles in the construction of our polyhedron. More precisely, for $t > t_c$, the 3-face H simplifies to a tetrahedron with vertices v_{132}, v_{213}, v_{321} and t_{32}, having one $\mathbb{C}$-planar and two $\mathbb{R}$-planar faces (see Figure 19). The whole polyhedron Π is then a cone over a union of two such tetrahedra, H and $J(H)$. Note that Π is non compact only for the critical values where $|t| = t_c$.

The side-pairings and cycles remain the same as earlier, removing those involving the 3-faces which have disappeared (namely T_1 and T_1' for $t > t_c$ and T_2 and T_2' for $t < -t_c$). In particular, there remains only one of the two integrality conditions from proposition 5.4.

Keeping these changes in mind, the arguments given above for small phase shift go through without any major modification. The main difference occurs for critical phase shift, since the hypotheses of the Poincaré polyhedron theorem include an extra verification at the cusps (see [FP]).

7 Comparison with Mostow's domains

In this section we comment on Mostow's fundamental domains for the groups $\Gamma(p,t)$ generated by R_1, R_2 and R_3 (for more details see [De]). The goal of his construction is to describe the Dirichlet fundamental domain centered at p_0. Mostow gives an explicit set of points in the orbit of p_0 that are supposed to describe all the faces of F, namely $R_i^{\pm 1}p_0$,$(R_iR_j)^{\pm 1}p_0$,$(R_iR_jR_i)^{\pm 1}p_0$ (a total of 24 points).

One then needs to prove that the corresponding 24 inequalities suffice. As explained in [M1], this can be done by using the appropriate version of the Poincaré polyhedron theorem, by verifying that the polyhedron bounded by the above 24 hypersurfaces has side pairings, compatible along the codimension two faces.

To explain what goes wrong in his agument, we observe that Mostow describes a polyhedron by giving each face of his k-skeleton, $0 \leq k \leq 3$, as the intersection of a number of bisectors (perhaps more than $4-k$ of them, some intersections not being transverse). Most of this skeleton is not geodesic, and in particular there are several instances of bigons, i.e. two different 1-faces with the same endpoints.

Mostow's verification that there are side pairings between the 3-faces is correct, but it is relatively easy to check numerically that, for some specific values of the parameters p and t, he missed some of the intersections between the 3-faces. This means that the polyhedron he uses is not simple, which makes it doubtful that it could be used in the context of a Poincaré polyhedron theorem.

Moreover, some of the verifications on the cycles of non totally geodesic 2-faces are incorrect, some of his 3-faces having (very tiny) extra intersections, that are easy to miss at first glance with coarse numerical experiments.

It turns out that for two of the groups (the ones with $p=5$ and large phase shift, namely $\Gamma(5,11/30)$ and $\Gamma(5,7/10)$), there are more faces in the Dirichlet domain than expected, corresponding to $(R_iR_j)^{\pm 2}p_0$ (see [De]). Although this might seem only like a minor correction, it illustrates the difficulty in using Dirichlet domains in complex hyperbolic geometry. Even though the construction is quite canonical (it depends only on the choice of the point p_0), bisector intersections are too complicated to be practical.

The complexity of Dirichlet domains is explained in part by the fact that none of its codimension two faces can ever be in a Lagrangian plane. Indeed, any two bisectors bounding faces of a Dirichlet domain are coequidistant, since their complex spines all contain p_0 (see section 2.5). If their intersection were to contain a Lagrangian plane L, the real reflection fixing L would preserve both complex spines, hence fix their intersection point, which is a contradiction.

In Mostow's Dirichlet domains, certain pairs of 2-faces are close to a Lagrangian plane, in the sense that their vertices are all contained in such an $\mathbb{R}$-plane. These two non totally geodesic faces wrap around a certain Lagrangian quadrilateral contained in the Dirichlet domain, forming some kind of droplet contained in a bisector having the Lagrangian as a meridian (see the pictures in [M1], Figure 14.4 in pg. 239, and [De]). One expects this phenomenon to be due to the rigid nature of Dirichlet domains, and indeed we get rid of such faces in our fundamental domains.

8 Appendix: list of faces and combinatorial structure of Π

We will now list the (proper) faces of Π; the inclusions are obvious because the 1- and 2-faces are determined by their vertices. The 1-faces are all geodesic segments, and the 2-faces are either $\mathbb{R}$- or $\mathbb{C}$-planar or unions of geodesics from p_{12} to a segment (the hexagon η is apart).

This contrasts strongly with Mostow's Dirichlet domain, where faces shaped like "bubbles" occur, in the form of distinct 1-faces having the same endpoints and of distinct 2-faces having the same boundary.

- The ten 3-faces:
  These are of three types (and five isometry classes): the core faces H and H', the tetrahedra T_1, T_1', T_2, T_2' (where $T_i^{(')}$ is the cone based on the triangle $\tau_{i1}^{(')}$) and the pentagonal pyramids P_1, P_1', P_2, P_2' (where $P_i^{(')}$ is the cone based on the pentagon $\pi_i^{(')}$).
- The twenty-five 2-faces:
  These are of three types (and ten isometry classes):
  - The right-angled hexagon $\eta = (s_{12}, \tilde{s}_{13}, s_{23}, \tilde{s}_{21}, s_{31}, \tilde{s}_{32})$ living in the intersection of bisectors B_1 and B_1'
  - Four $\mathbb{R}$-planar right-angled pentagons:
  $$\pi_1 = (t_{23}, s_{31}, \tilde{s}_{32}, s_{12}, t_{32})$$
  $$\pi_2 = R_1(\pi_1) = (t_{23}, \tilde{s}_{21}, s_{23}, \tilde{s}_{13}, t_{32})$$
  $$\pi_1' = J(\pi_1) = (t_{31}, s_{12}, \tilde{s}_{13}, s_{23}, t_{13})$$
  $$\pi_2' = J(\pi_2) = (t_{31}, \tilde{s}_{32}, s_{31}, \tilde{s}_{21}, t_{13})$$
  - Twenty triangles:

    The faces of T_1:
    $\tau_{11} = (t_{23}, s_{31}, \tilde{s}_{21})$ ($\mathbb{C}$-planar)
    $\tau_{12} = (t_{23}, s_{31}, p_{12})$ ($\mathbb{R}$-planar)
    $\tau_{13} = (t_{23}, \tilde{s}_{21}, p_{12})$ ($\mathbb{R}$-planar)
    $\tau_{14} = (p_{12}, s_{31}, \tilde{s}_{21})$ (generic)

    The faces of T_2:
    $\tau_{21} = (t_{32}, s_{12}, \tilde{s}_{13})$ ($\mathbb{C}$-planar)
    $\tau_{22} = (t_{32}, s_{12}, p_{12})$ ($\mathbb{R}$-planar)
    $\tau_{23} = (t_{32}, \tilde{s}_{13}, p_{12})$ ($\mathbb{R}$-planar)
    $\tau_{24} = (p_{12}, s_{12}, \tilde{s}_{13})$ (generic)

    The faces of T_1':
    $\tau_{11}' = (t_{31}, s_{12}, \tilde{s}_{32})$ ($\mathbb{C}$-planar)

$\tau'_{12} = (t_{31}, s_{12}, p_{12})$ ($\mathbb{R}$-planar)
$\tau'_{13} = (t_{31}, \tilde{s}_{32}, p_{12})$ ($\mathbb{R}$-planar)
$\tau'_{14} = (p_{12}, s_{12}, \tilde{s}_{32})$ (generic)

The faces of T'_2:
$\tau'_{21} = (t_{13}, s_{23}, \tilde{s}_{21})$ ($\mathbb{C}$-planar)
$\tau'_{22} = (t_{13}, s_{23}, p_{12})$ ($\mathbb{R}$-planar)
$\tau'_{23} = (t_{13}, \tilde{s}_{21}, p_{12})$ ($\mathbb{R}$-planar)
$\tau'_{24} = (p_{12}, s_{23}, \tilde{s}_{21})$ (generic)

And four triangles belonging to two pentagonal pyramids:
$\tau_{c1} = (t_{23}, t_{32}, p_{12})$ ($\mathbb{C}$-planar)
$\tau_{c2} = (t_{13}, t_{31}, p_{12})$ ($\mathbb{C}$-planar)
$\tau_{g1} = (s_{31}, \tilde{s}_{32}, p_{12})$ (generic)
$\tau_{g2} = (s_{23}, \tilde{s}_{13}, p_{12})$ (generic)

- The twenty-six edges (1-faces):

  These are the sixteen edges of the core part (6 for the hexagon, adding 5 for each of H and H') together with the ten edges joining the ten vertices of the core part to the cone point p_{12}.

- The eleven vertices (0-faces):

  These are the vertices of the hexagon: $s_{12}, \tilde{s}_{13}, s_{23}, \tilde{s}_{21}, s_{31}, \tilde{s}_{32}$ together with vertices t_{23}, t_{32} of H, t_{13}, t_{31} of H' and the cone point p_{12}.

References

[C] H. S. M. Coxeter; Regular Complex Polytopes. Cambridge University Press (1991).

[DM] P. Deligne, G. D. Mostow; *Monodromy of hypergeometric functions and non-lattice integral monodromy*. Publ. Math. IHES **63** (1986), 5–89.

[De] M. Deraux; *Dirichlet domains for the Mostow lattices*. Preprint.

[FK] E. Falbel, P.-V. Koseleff; *Rigidity and flexibility of triangle groups in complex hyperbolic geometry*. Topology **41**, no. 4 (2002), 767–786.

[FPa] E. Falbel, J. Paupert; *Fundamental domains for finite subgroups in $U(2)$ and configurations of Lagrangians*. Geom. Ded. **109** (2004), 221–238.

[FP] E. Falbel, J.R. Parker; *The Geometry of the Eisenstein-Picard modular group*. To appear in Duke Math. Journal.

[Gi] G. Giraud; *Sur certaines fonctions automorphes de deux variables*. Ann. ENS **38** (1921), 43–164.

[Go] W.M. Goldman; Complex Hyperbolic Geometry. Oxford Mathematical Monographs. Oxford Science Publications (1999).

[Mas] B. Maskit; Kleinian Groups. Springer-Verlag (1988).

[M1] G. D. Mostow; *On a remarkable class of polyhedra in complex hyperbolic space*. Pacific J. Mathematics **86** (1980), 171–276.

[M2] G. D. Mostow; *Generalized Picard lattices arising from half-integral conditions*. Inst. Hautes Études Sci. Publ. Math. **63** (1986), 91–106.

[Pi] E. Picard; *Sur les fonctions hyperfuchsiennes provenant des séries hypergéométriques de deux variables*. Ann. ENS III, **2** (1885), 357–384.

[S1] R. E. Schwartz; *Real hyperbolic on the outside, complex hyperbolic on the inside*. Invent. Math. **151** (2003), no. 2, 221–295.

[S2] R. E. Schwartz; *Complex hyperbolic triangle groups*. Proceedings of the International Congress of Mathematicians, Vol. II (Beijing, 2002), 339–349, Higher Ed. Press, Beijing, 2002.